Encoding of graded changes in spatial specificity of prior cues in human visual cortex

Yuko Hara and Justin L. Gardner

J Neurophysiol 112:2834-2849, 2014. First published 3 September 2014; doi:10.1152/jn.00729.2013

Journal of Neurophysiology publishes original articles on the function of the nervous system. It is published 12 times a year (monthly) by the American Physiological Society, 9650 Rockville Pike, Bethesda MD 20814-3991. ISSN: 0022-3077, ESSN: 1522-1598. Visit our website at http://www.the-aps.org/.

J Neurophysiol 112: 2834–2849, 2014.
First published September 3, 2014; doi:10.1152/jn.00729.2013.

Encoding of graded changes in spatial specificity of prior cues in human visual cortex

Yuko Hara and Justin L. Gardner
Laboratory for Human Systems Neuroscience, RIKEN Brain Science Institute, Wako, Saitama, Japan

Submitted 9 October 2013; accepted in final form 26 August 2014

Hara Y, Gardner JL. Encoding of graded changes in spatial specificity of prior cues in human visual cortex. *J Neurophysiol* 112: 2834–2849, 2014. First published September 3, 2014; doi:10.1152/jn.00729.2013.—Prior information about the relevance of spatial locations can vary in specificity; a single location, a subset of locations, or all locations may be of potential importance. Using a contrast-discrimination task with four possible targets, we asked whether performance benefits are graded with the spatial specificity of a prior cue and whether we could quantitatively account for behavioral performance with cortical activity changes measured by blood oxygenation level-dependent (BOLD) imaging. Thus we changed the prior probability that each location contained the target from 100 to 50 to 25% by cueing in advance 1, 2, or 4 of the possible locations. We found that behavioral performance (discrimination thresholds) improved in a graded fashion with spatial specificity. However, concurrently measured cortical responses from retinotopically defined visual areas were not strictly graded; response magnitude decreased when all 4 locations were cued (25% prior probability) relative to the 100 and 50% prior probability conditions, but no significant difference in response magnitude was found between the 100 and 50% prior probability conditions for either cued or uncued locations. Also, although cueing locations increased responses relative to noncueing, this cue sensitivity was not graded with prior probability. Furthermore, contrast sensitivity of cortical responses, which could improve contrast discrimination performance, was not graded. Instead, an efficient-selection model showed that even if sensory responses do not strictly scale with prior probability, selection of sensory responses by weighting larger responses more can result in graded behavioral performance benefits with increasing spatial specificity of prior information.

vision; attention; contrast; efficient-selection; gating

PRIOR INFORMATION about the relevance of particular spatial locations to a given visual perceptual task can guide spatial attention and thereby improve behavioral performance (Carrasco 2011; Pashler 1998). Prior information need not be all-or-none; multiple locations may possibly be relevant. Optimal use of prior information of increasing spatial specificity should result in graded behavioral improvements. That is, with fewer prior cued locations, the prior probability that any one cued location contains a target increases, and performance should be enhanced (Ciaramitaro et al. 2001). We asked about the neural mechanisms involved in the use of prior information of different spatial prior probabilities during a contrast-discrimination task by concurrently measuring behavioral performance and cortical activity with blood oxygenation level-dependent (BOLD) imaging. Computational modeling was used to assess how measured changes in cortical response could quantitatively account for behavioral performance.

Address for reprint requests and other correspondence: J. L. Gardner, Lab for Human Systems Neuroscience, RIKEN Brain Science Institute, 2-1 Hirosawa, Wako, Saitama 351-0198, Japan (e-mail: justin@brain.riken.jp).

We used a contrast-discrimination task so that we could test quantitative links between cortical activity and behavioral performance (Boynton et al. 1999; Zenger-Landolt and Heeger 2003). Because neural responses monotonically increase with contrast in early visual cortex (Albrecht and Hamilton 1982; Boynton et al. 1999; Gardner et al. 2005; Logothetis et al. 2001; Sclar et al. 1990; Tolhurst et al. 1981; Tootell et al. 1995), discriminating which stimulus had a higher contrast can be achieved by selecting the stimulus that evoked a larger response. Thus, increasing the slope of the relationship between contrast and response can improve contrast-discrimination performance by enhancing the difference in response to stimuli of different contrasts (Boynton et al. 1999; Foley and Legge 1981; response enhancement Legge and Foley 1980; Morrone et al. 2002; Nachmias and Sansbury 1974; Pestilli et al. 2011; Zenger-Landolt and Heeger 2003). Reducing the noise in the cortical representations can also improve performance by reducing the overlap in response distributions to different stimuli (Briggs et al. 2013; Cohen and Maunsell 2009; noise reduction Mitchell et al. 2009). In previous work, we found that neither of these two mechanisms of sensory enhancement alone can quantitatively account for behavioral performance improvements with attention in contrast-discrimination tasks (Pestilli et al. 2011). Instead, computational analyses suggested that efficient selection, implemented as a weighting of responses to each stimulus according to the magnitude of response, could account for improved behavioral performance. In the present study, we tested whether this "efficient-selection model" could quantitatively account for performance as the prior probability of spatial cues was systematically manipulated.

Unequal weighting of sensory evidence depending on attentional priority (Itti and Koch 2001) of particular locations or features is a common aspect of many theoretical approaches to attention (Desimone and Duncan 1995; Lee et al. 1999; Pelli 1985) and has an appealing interpretation in statistical decision-making accounts; the weights correspond to the prior probability (Eckstein et al. 2009) that a location is relevant. In this view, improvements in the sensitivity of sensory signals (i.e., sensory enhancement enabled via mechanisms such as response enhancement and noise reduction) play a less important role in improving behavioral performance compared with the preferential weighting of sensory signals from relevant locations. Since activity in the human visual cortex is known to be greater for cued locations (Kastner and Ungerleider 2000), one way to weight information from different locations according to relevance is to proportionally scale cortical responses with prior probability.

In this study, we found that although parametrically increasing prior probability resulted in graded improvements in behavioral performance, responses in early visual cortex did not strictly scale with prior probability. Whereas responses were smallest when prior probability was 25%, no significant difference in response magnitude was observed between locations with 50 and 100% prior probabilities. The cue sensitivity, which is the difference in response between cued and uncued locations, also did not significantly vary with prior probability. Finally, contrast sensitivity, which is the sensitivity to contrast differences quantified as the slope of the relationship between stimulus contrast and response, an important determinant of performance in contrast-discrimination tasks as explained above, did not vary with prior probability. However, a model of efficient selection, which used a nonlinear pooling mechanism to weight responses, could account for graded improvements in behavioral performance even though cortical responses did not strictly scale with prior probability.

MATERIALS AND METHODS

Subjects. Five human subjects (2 women and 3 men, ages 21–36, all but one naive to the purpose of the experiment) with normal or corrected-to-normal vision participated in the study. Experimental procedures were conducted with prior written consent from each subject and were approved in advance by the RIKEN Brain Science Institute Functional MRI Safety and Ethics Committee. Each subject participated in multiple functional experiments: one session for retinotopic mapping (1.5 h, consisting of at least 10 retinotopic scans lasting 4.5 min each) and five to seven sessions of the main experiment (2.0 h each, consisting of 1 or 2 localizer scans and 6–10 experiment scans lasting 7 min each).

Main experimental task. Subjects performed a contrast-discrimination task both inside and outside the scanner. The task was two-interval forced choice in which the subjects had to report the temporal interval for which one of four sinusoidal gratings had a higher contrast (Fig. 1). Subjects were instructed to view two 0.6-s presentations of the four grating stimuli (Stim1 and Stim2) separated by a 0.3-s interstimulus interval (ISI) while fixating on a central cross ($1° \times 1°$ visual angle and 1 pixel wide, 125.85 cd/m^2 outside, 4.05 cd/m^2 inside the scanner). The contrast at one and only one grating location (target, *top right* quadrant in Fig. 1) was slightly incremented in one of the temporal intervals (randomly chosen, Stim2 in Fig. 1). The location of this target grating was indicated by a small postcue (green line, 0.5° long and 5 pixels wide, stemming from the center of the fixation cross at a 45° diagonal) during the 1.5-s-long response interval (Resp in Fig. 1). Subjects were required to report the temporal interval in which the cued target had a higher contrast with a button press (by keyboard input of "1" or "2" outside the scanner, by 2 handheld buttons corresponding to either the "1st" or "2nd" interval inside the scanner). After the button press, subjects received feedback on their response by a color change of the fixation cross (green for correct, red for incorrect). The intertrial interval (ITI) was 1.0 s outside the scanner. To sample different BOLD response overlaps, inside the scanner, the ITI was randomized between 1.5 and 12.0 s in steps of 1.5 s. After running several hundred practice trials outside the scanner until performance stabilized, subjects performed an average of 1,016 and 1,191 trials outside and inside the scanner, respectively.

The main experimental manipulation in the task was the number of stimulus locations cued during the initial 1.0-s cue interval of each trial (Cue in Fig. 1). Before stimulus presentation, a cue consisting of small black lines (0.5° long and 5 pixels wide, 0.73 cd/m^2 outside, 0.13 cd/m^2 inside the scanner) appeared near fixation, pointing to either one, two, or four of the stimuli, always including the target location (Fig. 1, *A*, *B*, and *C*, respectively). These cues stemmed from

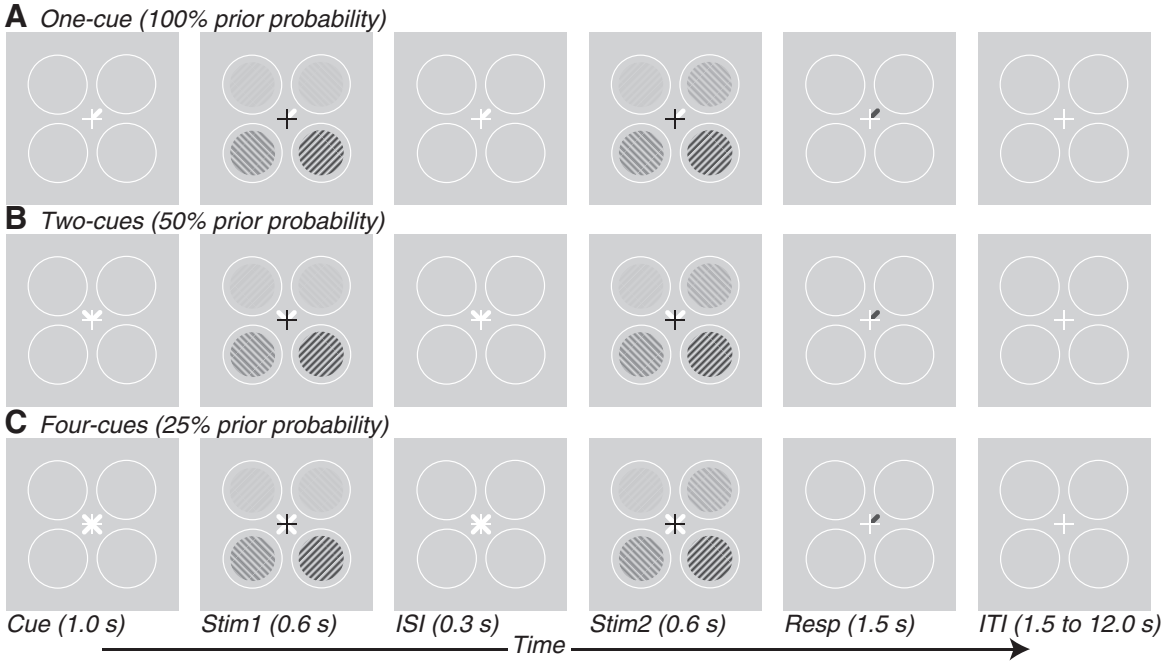

Fig. 1. Schematic diagram of the contrast-discrimination task in which spatial prior probability was manipulated by parametrically changing the number of cued locations. At the beginning of each trial (Cue interval), subjects were presented with valid cues pointing to either 1 (*A*), 2 (*B*), or all 4 (*C*) of the possible target locations, thus changing prior probability from 100 to 50 to 25%. The cues persisted while the stimulus, consisting of 4 contrast gratings, appeared in 2 temporal intervals (Stim1 and Stim2) separated by an interstimulus interval (ISI). In 1 of the 2 intervals (Stim2 in this figure), the contrast in 1 of the cued locations (target; *top right* quadrants in this figure) was slightly incremented. Following both stimulus presentation intervals, the cues were replaced by a green response postcue (appears dark gray in this figure) that indicated the target. Subjects reported with a button press in which interval the target contrast appeared greater (Resp). The intertrial interval (ITI) was fixed at 1.5 s for trials performed outside the scanner was and pseudorandomized between 1.5 and 12.0 s for trials performed inside the scanner.

the center of the fixation cross at 45° diagonals and persisted throughout fixation and stimulus presentation (Cue, Stim1, ISI, and Stim2).

The stimulus was an array of four sinusoidal gratings displayed on a gray background. The gratings were arranged at 6° eccentricity with one grating per visual quadrant. Each grating had a 3° radius, spatial frequency of 2 cycles/deg, and orientation orthogonal to its polar angle position and was displayed drifting at 1 Hz in opposite directions each interval. To reduce spatial uncertainty of the grating locations, the four possible target locations were indicated throughout the experiment by a white circular frame (6° eccentricity, 7.5° internal diameter). To reduce temporal uncertainty, the fixation cross color was changed to black during the two stimulus presentation intervals.

Contrast-discrimination performance was tested for three pedestal contrasts of 12.5, 25, and 50%. To avoid subjects being able to compare spatial locations rather than temporal intervals, the other three nontarget gratings were shown at an individually randomized contrast chosen from one of the pedestal contrasts. The randomization of contrasts at each location was also intended to minimize any differential adaptation effects (Dhruv et al. 2011; Dhruv and Carandini 2014; Kohn 2007; Ohzawa et al. 1982) that would bias the strength of responses at any particular location. However, responses within a trial might have been subject to rapid adaptation affects (Müller et al. 1999), which may make responses to different contrasts more similar over the course of a trial (Gardner et al. 2005).

For the target grating, a 1-up-2-down staircase (Levitt 1971) was used to set the increment in contrast (Δc), which was added to the pedestal contrast in one of the temporal intervals. Independent and pseudorandomly interleaved staircases were used for each cue condition and each pedestal contrast to maintain task performance around 70.7% for all conditions. The independent staircases balanced task difficulty across all conditions and all pedestal contrasts so that subjects would always be performing the task at a near-threshold level, eliminating any potential confound with task difficulty between conditions.

Contrast-discrimination function. Contrast-discrimination task performances between different cue conditions were evaluated using their contrast-discrimination functions. Contrast-discrimination functions defined the relationship between each pedestal contrast (c) and the increment in contrast (Δc) required at each pedestal contrast to obtain threshold-level performance. Contrast-discrimination functions were computed separately for each cue condition from the behavioral data as follows. For each pedestal contrast and cue condition, a maximum likelihood procedure (Wichmann and Hill 2001) was used to fit subject responses with a Weibull function (Weibull 1951):

$$p(\Delta c) = \left(\frac{1}{2} - \delta\right)\left(1 - e^{-\left(\frac{\Delta c}{\varepsilon}\right)^m}\right) + \frac{1}{2}, \quad (1)$$

where $p(\Delta c)$ is the probability of being correct given a contrast increment of Δc, δ is the lapse rate, ε is the Δc for which the probability correct reaches 63% of the difference between chance and maximal performance, and m is the slope of the psychometric function. Subjects performed on average 238 trials per psychometric function, sufficient for accurate determination of discrimination thresholds (Kontsevich and Tyler 1999), the main measure of interest. From the fitted Weibull function, we computed the discrimination threshold as the contrast increment Δc that would give a correct rate $p(\Delta c)$ of 76% for that particular cue condition and pedestal contrast. Contrast-discrimination functions were then constructed for each cue condition by plotting these discrimination thresholds as a function of pedestal contrast (Fig. 2).

Stimulus presentation. Outside the scanner, the visual stimuli were presented on a Dell Trinitron 21-in. flat-screen CRT monitor (Dell, Round Rock, TX) with a resolution of 1,280 × 960 pixels and a 100-Hz refresh rate placed at a distance of 50.5 cm from the subject's eyes to obtain a field of view of 43° × 32°. Inside the scanner, subjects used an adjustable mirror system to view an image that was rear-projected by an Avotec Silent Vision 6011 LCD projector (Avotec, Stuart, FL) onto a screen placed inside the bore of the magnet at a distance of 38.5 cm to obtain a minimum field of view of 50° × 20°. The projector had a resolution of 800 × 600 pixels and a 60-Hz refresh rate. Both displays were calibrated to a linearized gamma using a Topcon SR-3A-L1 Spectroradiometer (Topcon, Tokyo, Japan). We dynamically adjusted the 10-bit gamma table to achieve the best luminance resolution possible (while maintaining linearized output) for displaying each set of gratings. All stimuli were generated using MATLAB (The MathWorks, Natick, MA) and MGL (http://justingardner.net/mgl).

Eye position measurements. An EyeLink 1000 eye tracking system (SR Research, Mississauga, ON, Canada) was used outside the scanner, and iView eye tracking software (SensoMotoric Instruments, Teltow, Germany) coupled to an external camera (Avotec) was used inside the scanner to confirm that subjects maintained fixation throughout the task. Both systems recorded corneal reflections of an external infrared light source and tracked the center of the pupil. A

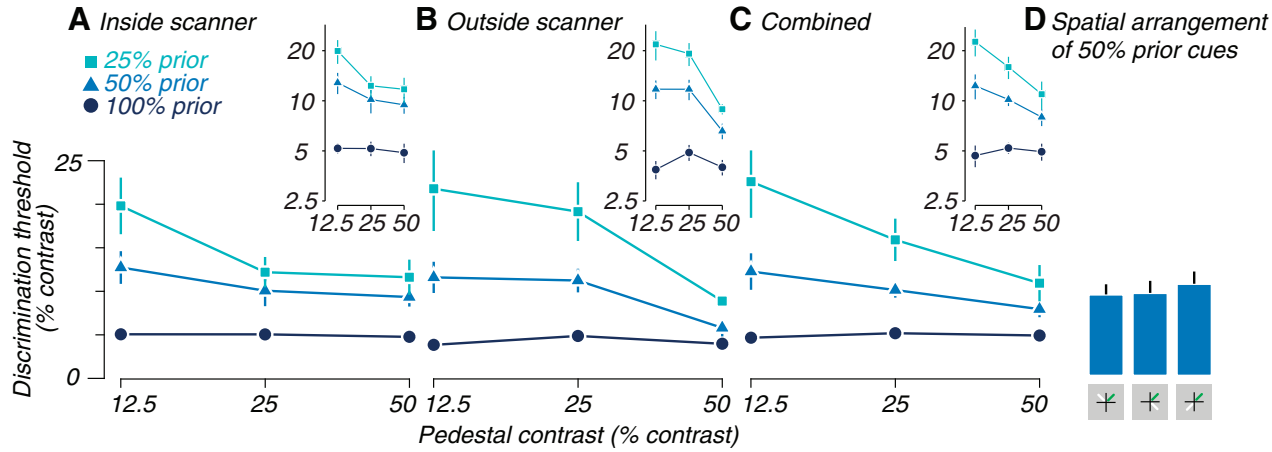

Fig. 2. Contrast-discrimination functions averaged across all subjects show graded improvement in performance with increasing prior probability. Discrimination thresholds were computed separately for trials performed inside (*A*) and outside (*B*) the scanner, as well as across all trials combined (*C*). Contrast-discrimination functions for the 100 (dark blue lines), 50 (medium blue lines), and 25% prior probability conditions (light blue lines) were plotted on a semi-log axis. *Insets* show the same set of contrast-discrimination functions on a log-log axis. *D*: discrimination thresholds for different spatial arrangements of the 2 cues in the 50% prior probability condition did not show significant differences (means across pedestal contrasts). Error bars indicate SE of means across subjects. Error bars for the 100% prior probability condition in *A–C* are smaller than the size of the symbols.

brief calibration was performed before each continuous session outside the scanner and before at least every other functional scan inside the scanner. Eye tracking setup was successful for all sessions outside the scanner. However, due to physical constraints imposed by subject and mirror positioning inside the scanner, the eye tracker could only be successfully set up in 44% of scanner sessions. Subjects fixated on a central yellow dot and then on subsequent yellow dots that appeared 5° to the left, right, above, and below the center of the screen. This calibration data was used to perform an affine transformation of the acquired eye tracking data to the position of the eye in degrees of visual angle.

For trials performed outside the scanner, the mean eye position during stimulus presentation (Stim1 and Stim2 combined in Fig. 1) was calculated for each cue condition. Blink artifacts were removed (100 ms before and after each blink). Eye positions were analyzed for differences across cue conditions (separately for each cue configuration, i.e., actual stimuli cued). For trials performed inside the scanner, the subject's eye position was monitored by the experimenter. One subject had complete eye tracking and calibration data from inside the scanner, which was analyzed similarly to the data acquired outside the scanner.

MRI acquisition and preprocessing. MRI data were acquired on a Varian Unity Inova 4 Tesla whole body MRI system equipped with a head gradient system (now Agilent Technologies, Santa Clara, CA). High-resolution three-dimensional (3-D) anatomic MR images (T1 weighted) were acquired with a birdcage radiofrequency (RF) coil (Nova Medical, Wilmington, MA). Functional data (T2* weighted) were acquired using a volume RF coil to transmit and a four-channel receive array (Nova Medical). Sponge padding was used to restrict head motion. The subject's respiration was monitored using a pressure sensor, and the heartbeat was measured with a pulse oximeter. These data were later used along with RF pulse timings to correct the functional data for physiological fluctuations.

For each subject we acquired high-resolution 3-D anatomic images of the brain ("canonical anatomy") in a separate scanning session, which could be used for segmentation of the gray matter, surface generation, and alignment with data from separate functional sessions. In general, we collected two T1-weighted images (MPRAGE TR 13 ms, TI 500 ms, TE 7 ms, flip angle 11°, voxel size $1 \times 1 \times 1$ mm, matrix $256 \times 256 \times 180$) and one T2-weighted image (FLASH TR 13 ms, TE 7 ms, flip angle 11°, voxel size $1 \times 1 \times 1$ mm, matrix $256 \times 256 \times 180$). The two T1-weighted images were averaged then divided by the T2-weighted image to reduce global inhomogeneities in image contrast (Van De Moortele et al. 2009). The public domain software FreeSurfer (http://surfer.nmr.mgh.harvard.edu) was then used to segment the gray-matter from the white-matter and generate surfaces (Dale et al. 1999). Flattened representations of the cortical surface were used for drawing regions of interest, including visual areas and subregions thereof which contained responses to a specific stimulus grating. These regions of interest were constrained to voxels that intersected the gray matter. Analyses were all conducted on the original untransformed data and the surfaces and flattened representations were used solely for data visualization.

Each functional experimental session (including retinotopy scans) included a 3-D T1-weighted anatomical image for registration with the canonical anatomy and multiple T2*-weighted functional scans. The anatomic image [magnetization-prepared rapid acquisition gradient-echo (MPRAGE): TR 11 ms, TI 500 ms, TE 6 ms, flip angle 11°, voxel size $1.72 \times 1.72 \times 1.72$ mm, matrix $128 \times 128 \times 64$] was typically taken in the same orientation as the functional images. These anatomic images were used with an automated procedure (Nestares and Heeger 2000) to find the best affine transformation to align the images from each session to the canonical anatomy. BOLD changes (Ogawa et al. 1990) in image intensity were measured using T2*-weighted gradient recalled multi-shot echo-planar imaging with sensitivity encoding (SENSE) (Pruessmann et al. 1999). For retinotopic mapping, 21 slices were acquired with a volume acquisition time after SENSE acceleration of 1,572 ms (2-shot, SENSE acceleration factor 2, TE 25 ms, flip angle 55°, voxel size $3 \times 3 \times 3$ mm, matrix 64×64). For the main experiment, 16 slices were acquired with a volume acquisition time after sense acceleration of 1,200 ms (2-shot, SENSE acceleration factor 2, TE 25 ms, flip angle 51°, voxel size $3 \times 3 \times 3$ mm, matrix 64×64). Oblique slices were chosen to maximally cover the occipital visual areas, approximately perpendicular to the calcarine sulcus.

Preprocessing for functional data in each session were performed in the following order: corrections for physiological fluctuations, SENSE reconstruction, motion compensation, detrending, and then high-pass filtering. Cardiac and respiratory fluctuations of image intensity were removed using a retrospective estimation and correction procedure (Hu et al. 1995). For the SENSE reconstruction, a mask image was manually drawn around all signal voxels and used to improve image reconstruction quality (Pruessmann et al. 1999). Following reconstruction, standard procedures were used for motion compensation (Nestares and Heeger 2000). Time courses were then linearly detrended and high-pass filtered (cutoff of 0.01 Hz) to remove low temporal frequency drifts. BOLD signal change (%signal change) was computed by dividing the time course of each voxel by its mean intensity over the course of each scan.

Retinotopy and localizer. Visual fields were determined based on a retinotopy performed in a separate scanning session. High-contrast radial checkerboard patterns were presented as either an expanding or contracting ring or a 90° rotating wedge. Each scan consisted of 10.5 cycles (25.2 s per cycle) of the ring expanding/contracting or the wedge completing a full rotation with a sampling rate of 16 volumes per cycle (168 volumes per scan). The first half-cycle of each scan was discarded from the analysis. Each session consisted of four scans of the ring stimulus (2 expanding and 2 contracting) and at least six scans of the rotating wedge stimulus (3 clockwise and 3 counterclockwise), interleaved. Time courses from all scans were time-shifted 2 or 4 s, and time courses from contracting ring and counterclockwise wedge scans were time-reversed and averaged with the time courses for expanding and clockwise wedge scans, respectively. The averaged ring and wedge responses were Fourier transformed to obtain the response amplitude, phase, and coherence (normalized amplitude) at the stimulus frequency. Visual fields were defined according to published criteria (Gardner et al. 2008; Wandell et al. 2007).

To identify the voxels corresponding to each of the four grating locations, we used a stimulus localizer scan. These scans were performed in the beginning and/or end of each functional session so that each subject completed a total of 8–15 localizer scans in total across all experimental sessions. The localizer stimulus consisted of flickering sinusoidal gratings (identical in size and parameters to those of the experimental task) that were presented sequentially; the gratings were on for 12 s and then off for 12 s at each location and were temporally staggered so that each sequential location was turned on 6 s after the previous one. This 24-s stimulus cycle was repeated 10 times during each localizer scan. A correlation analysis was performed on the measured data, and voxels were included in regions of interest if the response had a coherence value >0.5 for visual areas V1–4 and 0.3 for V3A. Responses to each individual grating location were identified according to the phase of the response. Mislocalized voxels whose phase did not correspond with the rest of the voxels in the same visual area, probably due to partial voluming artifacts, were removed from the analysis. Using responses localized to each grating, we were able to separately analyze responses to each grating based on both the image contrast of that grating and whether it was cued or not cued in each of the three cue conditions.

Contrast-response function. To compute contrast-response functions, a deconvolution analysis (for details see Gardner et al. 2005) was used to determine the mean hemodynamic response to the grating in each location. The average time course in each visual area for each grating location was computed, and the responses following stimulus presentation for 15 s were calculated assuming linear summation for

responses that had temporally overlapped. These responses were calculated separately for each combination of pedestal contrast (12.5, 25, and 50% contrast), cue condition (25, 50, and 25% prior probability conditions), and whether the location had been cued or uncued (note that in the case of 25% prior probability where all locations were cued, there was no uncued condition). This lead to a total of 15 conditions (3 pedestals × 5 conditions, where the 5 conditions comprise conditions in which the location was cued in all 3 prior probability conditions plus conditions in which the location was not cued in 2 of the prior probability conditions). The responses for each of the 15 conditions were then averaged across the 4 locations. A gamma function was fit to this deconvolved response, and the magnitude of response was determined by the amplitude of this function. These response magnitudes were then averaged across subjects and plotted as a function of grating contrast to yield the contrast-response functions for each visual area and each cue condition (Fig. 3).

For each location, a single response was used to average the cortical activity over the two stimulus intervals because the ISI in our task design was relatively short (0.3 ms) and the contrast shown in the two stimulus intervals were either the same (for nontargets) or offset by only a small change in contrast (for targets). To account for the small change in contrast that took place during one of the two stimulus intervals at the target location, the contrast responses for cued locations (Fig. 3, solid lines) were offset along the *x*-axis by the average contrast increment across all trials multiplied by 0.5 (since the increment occurred in 1 of 2 intervals) and were scaled by the prior probability (1, 0.5, or 0.25, since increment occurred in all, one-half, or one-quarter of the locations averaged, respectively).

Responses may be artificially inflated due to poststimulus modulations (Sergent et al. 2011) at cued target locations, so we adjusted responses to account for this effect. For the 50 and 25% prior probability conditions, we calculated responses at the cued locations separately for whether they were later the target for discrimination (cued target) or not (cued nontarget). We then used the cued nontarget response as the estimated responses to cued locations because it would not be corrupted by poststimulus modulations of the sort reported by Sergent et al. (2011). For the 100% prior probability condition there was no cued nontarget location by definition, so we estimated the size of the poststimulus modification as the average difference between cued target and cued nontarget responses for the 25 and 50% prior probability conditions (assuming that poststimulus modification for the 100% prior probability condition would be similar in magnitude to other prior probability conditions) and subtracted this from the 100% cued target response on a subject-by-subject basis. This procedure made quantitative but not qualitative differences in the estimated responses and did not change any conclusions.

Efficient-selection model. We fit a model for the selection of sensory responses to the measured contrast-discrimination and measured contrast-response functions, which we have described in detail previously (Pestilli et al. 2011). Briefly, the model simulated 10,000 trials in which simulated responses based on the measured contrast-response functions from all four locations were combined using a pooling rule (*Eq. 2*), and then discrimination thresholds were computed that would yield a performance equivalent to that measured by the contrast-discrimination function ($d' = 1$, 76% correct assuming unbiased responses). On each simulated trial, the response for each grating location was pulled from a Gaussian distribution with its mean set to the response based on the measured contrast-response functions for the particular grating contrast and cue condition, and the standard deviation (σ) was a model parameter. Intermediate values for contrast response were estimated using linear interpolation of the measured contrast-response functions, the slopes and intercepts of which were included as model parameters. These four response values were combined using the following equation:

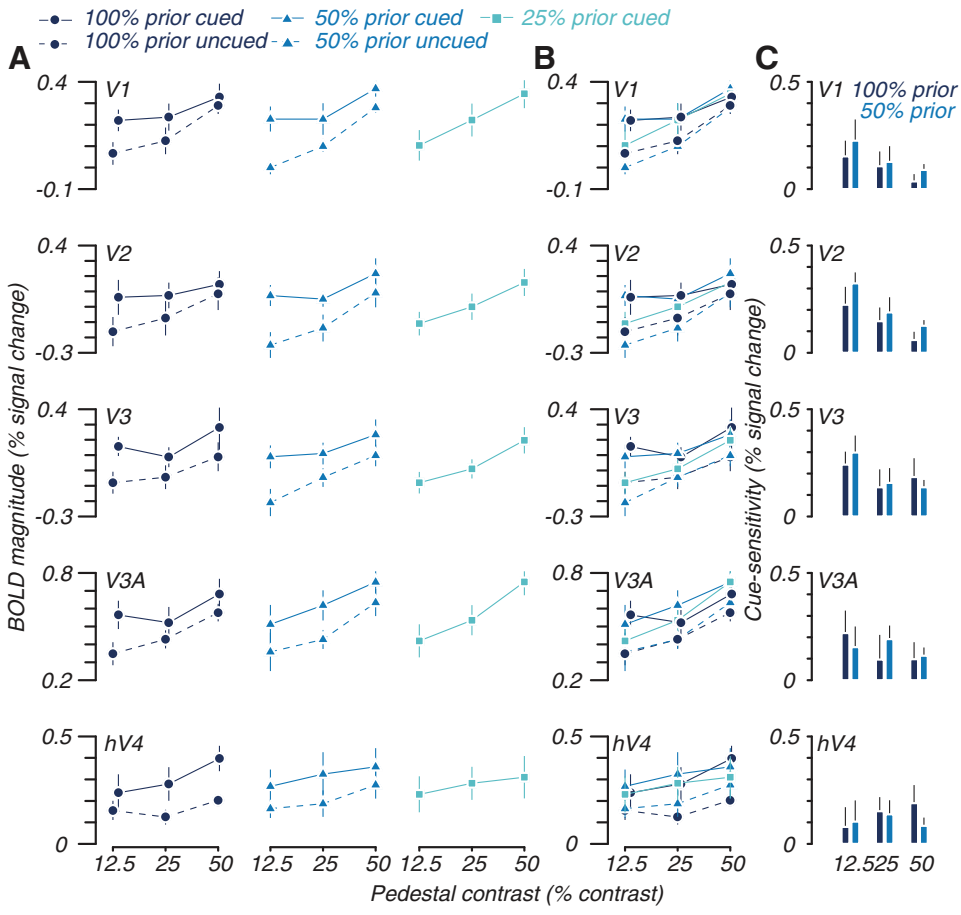

Fig. 3. Contrast-response functions averaged across all subjects show that cue sensitivity is positive and similar for the 100 and 50% spatial prior probability conditions in all visual areas. Blood oxygen level-dependent (BOLD) response magnitudes were greater in cued (solid lines) than uncued locations (dashed lines) for all prior probability conditions (*A*). *B* shows plots of the same data as in *A* on a single graph for direct comparison. Note that the data points for cued locations (solid lines) were shifted right to account for the threshold contrast increment (see MATERIALS AND METHODS, *Contrast-response function*, for details). *C*: cue sensitivity, which is the difference in cued and uncued response magnitudes (averaged across pedestal contrasts), are shown for the 100 (dark blue bars) and 50% prior probability conditions (medium blue bars). Error bars indicate SE of means across subjects.

$$R = \frac{1}{4}\sqrt[k]{\sum_{i=1}^{4} r_i^k}, \quad (2)$$

where R is the pooled response, r_i is the response at location i, and k is a parameter that smoothly varied the operation from averaging the response across the four locations ($k = 1$) to maximizing ($k = \infty$). k was used as a model parameter. On each simulated trial, pooled responses were computed for each temporal interval (one of which included a contrast increment at the target location), and the response that had the larger pooled magnitude was taken as the choice of the simulated observer. If this choice matched the interval in which the contrast increment appeared, the trial was marked correct. Model parameters σ and k and the slope and intercept of the contrast-response functions were adjusted until the model produced the best fit to the measured contrast-response and measured contrast-discrimination data in the least-squares sense. The model therefore had either 8 or 9 parameters (depending on whether cued and uncued locations were assumed to have the same σ or not; see RESULTS for details) to fit 24 data points.

RESULTS

Graded contrast-discrimination performance with prior probability. We tested subjects' ability to discriminate contrasts while varying the prior probability that any given location contained the stimulus to be discriminated. Subjects viewed four sinusoidal grating stimuli of different contrasts (chosen from 12.5, 25, and 50%) that appeared in two brief temporal intervals (Fig. 1, see MATERIALS AND METHODS, *Main experimental task*, for more details). In one of the temporal intervals, a single grating stimulus (target) was presented with a threshold increment in contrast. All other grating stimuli were presented with the same contrast in both temporal intervals. During the response interval, the target was postcued with a green line segment near fixation and the subjects were asked to report with a button press in which temporal interval the target grating had appeared with a higher contrast.

The key manipulation used to vary prior probability across trials was to change the number of grating locations cued in advance that could potentially contain the target. This was done by cueing with a white line segment near fixation either one, two, or four possible locations during the cue interval at the beginning of each trial (Fig. 1, first temporal interval of *A*, *B*, and *C*, respectively). The target grating was always one of the locations cued. Therefore, the prior probability that any cued location would be the target was varied from 100 to 50 to 25% probability as more locations were cued. The number of prior cues as well as the pedestal contrast of the target were pseudorandomly interleaved across trials. Task difficulty was maintained to be the same across all these conditions by running independent staircases to adaptively determine contrast increments that maintained threshold contrast-discrimination performance separately for each condition.

Behavioral performance improved in a graded fashion as a function of prior probability ($P < 0.001$ for main effect of prior probability, 3-way ANOVA over prior probability, pedestal contrast, and where the trials were performed, inside or outside the scanner). Performance was best (smallest discrimination thresholds) when prior probability was set to 100% by only cueing the target location in advance (Fig. 2, dark blue curves, 1 cue). Decreasing prior probability to 50% (Fig. 2, medium blue curves, 2 cues) resulted in worse performance compared with 100% prior probability ($P < 0.001$, paired *t*-test across subjects and pedestal contrasts), and thresholds for the 25% prior probability condition were worse than for the 50% prior probability condition ($P < 0.001$, paired *t*-test). Performance was 2.1- and 3.3-fold worse in the 50 and 25% prior probability conditions, respectively, compared with the 100% prior probability condition. The overall pattern of behavioral performance did not vary significantly whether the task was performed inside or outside the scanner; therefore, behavioral analysis was performed on all trials combined (Fig. 2, *A*, *B*, and *C*, respectively; $P > 0.9$ for where the trials were performed, 3-way ANOVA; see above). Subject eye positions were steady across all cue conditions ($P > 0.78$ and $P > 0.30$ in the *x*- and *y*-directions, respectively, for all possible pairs of cue conditions, Student's *t*-test). Inside the scanner, eye position measurements were generally of insufficient quality for statistical analysis; however, an analysis of one subject's complete data showed no significant difference in eye position for any pair of cue conditions at a Bonferroni-corrected *P* value of 0.05.

Behavioral performance did not vary according to the spatial arrangement of the two cued gratings in the 50% prior probability condition (Fig. 2*D*). Cued gratings could be in opposite hemifields, the same hemifield, or diagonally across from each other (Fig. 2*D, bottom*). These conditions therefore might be more or less attentionally demanding depending on whether attention can easily encompass locations across visual fields (Abrams et al. 2012; Alvarez and Cavanagh 2005; Alvarez et al. 2012 He et al. 1996). However, in our data, discrimination thresholds did not differ significantly according to the position of the cued, nontarget location relative to the target (Fig. 2*D*; $P > 0.3$ for main effect of spatial arrangement of the 2 cues in the 50% prior probability condition, 3-way ANOVA over spatial arrangement of the 2 cues, pedestal contrast, and where the trials were performed).

Contrast-discrimination performance was also affected by the target pedestal contrast ($P < 0.0016$ for main effect of pedestal contrast, 3-way ANOVA over prior probability, pedestal contrast, and where the trials were performed). Whereas, typically, contrast-discrimination performance gets worse (thresholds increase) as contrast is increased (Legge and Foley 1980; Nachmias and Sansbury 1974), performance for our task became better as a function of contrast, particularly for the 25 and 50% prior probability conditions in which four and two gratings were cued in advance, respectively. Averaged across the 25 and 50% prior probability conditions, thresholds were ~1.3 and 1.8 times better at 25 and 50% contrasts, respectively, than at 12.5% contrast. Our model of efficient selection (Pestilli et al. 2011) can successfully account for the pattern of results found in these data by taking into account the distracting effect of the nontarget contrasts in each trial (see RESULTS, *Efficient-selection model predictions for distractor effects*).

BOLD magnitude, cue sensitivity, and contrast sensitivity do not strictly scale with prior probability. Simultaneously with the behavioral measurements reported above, we recorded cortical responses as measured by BOLD imaging at each grating location to determine the effect of cue condition on each response. Cortical responses were first separated into responses associated with each visual area (V1–4 and V3A) as determined by retinotopic criteria measured in a separate scanning session (see MATERIALS AND METHODS, *Retinotopy and localizer*). Locations within each visual area were then identi-

fied with the use of a stimulus localizer sequence that was run either once or twice during each of the five-to-seven scanning sessions used for the main experiment for each subject. We then computed the average response, assuming that temporally overlapping responses sum linearly (Boynton et al. 1996), to each trial type (either the 100, 50, or 25% prior probability conditions), sorted by contrast of the grating at that location and whether the grating was cued or uncued. Responses across the four locations within each visual area were then averaged, and the magnitude of response was reported (Fig. 3*A* shows sorted responses for different trial types in separate columns, and Fig. 3*B* displays all responses in Fig. 3*A* on the same axis).

Unlike behavioral performance, magnitude of cortical responses did not strictly scale with prior probability (Fig. 3*A*, compare 1st, 2nd, and 3rd columns). Despite prior probability being halved from 100 to 50%, cued locations had similar response magnitudes (0.26 vs. 0.27, 0.09 vs. 0.11, 0.18 vs. 0.14, 0.59 vs. 0.63, and 0.30 vs. 0.32% signal change in V1-hV4 and V3A, respectively, averaged across all pedestal contrasts) that were statistically indistinguishable in all visual areas studied ($P > 0.28$ in V1–4 and V3A, uncorrected for multiple comparisons, paired *t*-test over subjects). Similarly, on a subject-by-subject basis, only 12% of subject visual areas (3 of 25) showed a significant difference ($P > 0.05$, *t*-test over stimulus presentations) for cued responses when the spatial prior probability was reduced from 100 to 50%. For the three subject visual areas that had shown significant differences, one showed an increase and two a decrease as prior probability increased from 50 to 100%. Similarly, uncued responses showed no statistical significance between the 100 and 50% prior probability conditions in all visual areas studied ($P \geq 0.06$ in V1–4 and V3A, paired *t*-test; see above). If anything, there was a counterintuitive trend toward less suppression of the uncued responses in the 100% prior probability condition (0.16 vs. 0.13, −0.05 vs. −0.10, −0.01 vs. −0.05, 0.45 vs. 0.47, and 0.16 vs. 0.21% signal change in V1-hV4 and V3A, respectively, averaged across all pedestal contrasts). On a subject-by-subject basis, only 32% of subject visual areas (8 of 25) showed a significant difference ($P < 0.05$, *t*-test over stimulus presentations) with 6 showing, counterintuitively, less suppression when prior probability was 100%. There was a slight decrease in activity from 50 to 25% prior probability for cued locations (0.27 vs. 0.22, 0.11 vs. 0.02, 0.14 vs. 0.04, 0.63 vs. 0.57, and 0.32 vs. 0.27% signal change in V1-hV4 and V3A, respectively, averaged across all pedestal contrasts) that reached statistical significance in V2 and V3 ($P < 0.01$, paired *t*-test, see above) but not in other areas ($P \geq 0.14$). Thus BOLD magnitudes did not strictly scale with prior probability.

Changing prior probability also did not significantly change cue sensitivity, the difference between cued and uncued responses (Fig. 3*C*). Cue sensitivity was positive in all visual areas (indicating a larger response for cued locations) but was similar in magnitude regardless of whether prior probability was 100 or 50% (0.10 vs. 0.15, 0.14 vs. 0.21, 0.19 vs. 0.20, 0.45 vs. 0.47, and 0.14 vs. 0.11% signal change in V1–4 and V3A, respectively, averaged across all pedestal contrasts). The differences were not statistically significant ($P > 0.13$, paired *t*-test) in all areas except in V2 ($P = 0.033$), where cue sensitivity was, paradoxically, greater with 50 than 100% prior probability. On a subject-by-subject basis, only 16% of subject visual areas (4 of 25) showed a significant difference ($P < 0.05$, *t*-test over stimulus presentations) between the 100 and 50% prior probability conditions, with all four showing, paradoxically, greater cue sensitivity in the 50% prior probability condition. Thus cue sensitivity was not graded with prior probability. Note that because the 25% prior probability condition lacked any uncued locations, we could not evaluate cue sensitivity for this condition.

The relationship between contrast and response did not show graded changes with prior probability. For contrast discrimination, the slope of the relationship between contrast and response is critical; the higher the slope, the larger the difference in response evoked for the same change in contrast, which would be expected to result in greater discriminability of contrast (Boynton et al. 1999; Foley and Legge 1981; Legge and Foley 1980; Morrone et al. 2002; Nachmias and Sansbury 1974; Pestilli et al. 2011; Zenger-Landolt and Heeger 2003). Systematic changes in the slope of contrast response then could potentially account for graded behavioral performance with prior probability. To quantify the degree of sensitivity to grating contrast, we defined contrast sensitivity as the slope of the contrast-response function plotted on a linear (or semi-log) axis and compared it across the different prior probability conditions. BOLD responses increased with contrast for all visual areas (Fig. 3*A*, slopes of contrast-response functions; $P < 0.01$ in V1 and hV4, $P < 0.02$ in V2 and V3, $P = 0.06$ in V3A, Student's *t*-test for contrast sensitivity >0), thus giving positive values to contrast sensitivity as expected from the monotonically increasing relationship between contrast and response (Albrecht and Hamilton 1982; Boynton et al. 1999; Gardner et al. 2005; Logothetis et al. 2001; Sclar et al. 1990; Tolhurst et al. 1981; Tootell et al. 1995). Contrast sensitivities did not show significant differences with prior probability in all visual areas, regardless of whether the slope was calculated on a linear or semi-log axis ($P \geq 0.25$ for main effect of prior probability on slopes of cued and uncued responses calculated on both linear and semi-log axes, 2-way ANOVA over prior probability and subjects). These results agree with earlier reports finding no difference in BOLD-measured contrast sensitivity in early visual areas with attention (Buracas and Boynton 2007; Li et al. 2008; Murray 2008; Pestilli et al. 2011) and extend them to a range of spatial prior probabilities. Thus graded behavioral performance was not due to graded changes in contrast sensitivity.

The above-reported features of contrast response as a function of prior probability were robust to the criteria by which we selected voxels for inclusion in the analysis. As reported in MATERIALS AND METHODS. *Retinotopy and localizer*, we defined the response to each target in each visual area using data from a localizer scan using a fairly strict cutoff (coherence = 0.5 for V1-hV4 and 0.3 for V3A). If we made the cutoff stricter (coherence = 0.7), only areas V1-V3 had voxels that passed the cutoff. These responses still increased with contrast, albeit with marginal significance in V2 and V3 ($P < 0.01$ in V1, $P \leq 0.085$ in V2–3 for the linear scale and $P < 0.01$ in V1, $P \leq 0.13$ in V2–3 for the semi-log scale, Student's *t*-test for contrast sensitivity >0). Contrast sensitivity did not vary significantly with prior probability ($P \geq 0.34$ in V1, $P \geq 0.15$ in V2, and $P > 0.09$ in V3 for main effect of prior probability on slopes of cued and uncued responses calculated on both linear and semi-log axes, 2-way ANOVA over prior probability and subjects). Reducing prior probability from 100 to 50% did not

significantly change response magnitude at cued (0.28 vs. 0.32, 0.12 vs. 0.18, and 0.12 vs. 0.16% signal change, averaged across pedestal contrasts, with $P = 0.1$, 0.28, and 0.34 for V1–3, respectively, uncorrected for multiple comparisons, paired *t*-test over subjects) or uncued locations (0.15 vs. 0.16, −0.02 vs. −0.10, and −0.07 vs. −0.09% signal change with $P = 0.62$, 0.053, and 0.6 for V1–3, respectively, paired *t*-test; see above). Similarly, if we made the cutoff less strict (coherence = 0.3), responses in V1–4 still increased with contrast (all $P < 0.04$, Student's *t*-test; see above), but contrast sensitivity did not vary significantly with prior probability (all $P \geq 0.19$ for main effect of prior probability, 2-way ANOVA; see above), and response magnitudes did not vary significantly between the 100 and 50% prior probability conditions at cued (0.18 vs. 0.21% signal change with $P = 0.094$ for V1, and 0.04 vs. 0.05, 0.15 vs. 0.13, and 0.58 vs. 0.59% signal change with all $P \geq 0.6$ in V2–4, respectively, paired *t*-test; see above) or uncued locations (−0.08 vs. −0.13 and 0.01 vs. −0.04% signal change with $P = 0.051$ and 0.10 in V2 and V3, respectively, and 0.13 vs. 0.11 and 0.46 vs. 0.48% signal change with all $P \geq 0.49$ in V1 and hV4, respectively, paired *t*-test; see above). Thus changing the voxel selection criteria did not change the main finding that early visual areas displayed contrast-sensitive responses that did not significantly track prior probability in either sensitivity (slope of contrast response) or magnitude at cued and uncued locations.

Subjects could use prior probability to improve response preparation time; at higher prior probabilities, there is less uncertainty as to which target they should respond about before the response postcue is presented at the end of the trial, and they could therefore respond more quickly. Correspondingly, we found reaction times were on average shorter for the 100 compared with 50% prior probability condition (difference of 215.6 ms, $P < 0.05$, *t*-test over subjects) and likewise for the 50 compared with 25% prior probability condition (difference of 71.65 ms, $P < 0.05$). Although these results support the behavioral result that subjects' behavioral performance tracks prior probability, it also raises a potential confound in our measured responses: subjects may stop attending to stimuli earlier (Kiani et al. 2008) with higher prior probability such that estimated responses for higher probability conditions may be artificially low.

To investigate the effect of such a confound on our measurements, we corrected for the potential decrease in response magnitude resulting from a reduction in attended duration with increasing prior probabilities. For the correction, we first computed cue selectivity, the difference in response between cued targets and uncued nontargets, and then scaled cue selectivity according to the estimated reduction in attended duration relative to the longest estimated attended duration for each subject. That is, we assumed that the 25% prior probability condition had the longest attended duration and that the other prior probability conditions had lower attended durations. Thus the ratio of the 25% prior probability reaction times to the 50 and 100% prior probability reaction times (calculated on a subject-by-subject basis) was used as a scaling factor to increase the cue selectivity magnitude for the 50 and 100% prior probability conditions. The resulting scaled cue selectivity was added back to the 50 and 100% prior probability uncued measured response magnitudes, and those values were used as the corrected cued responses. The resulting corrected response magnitude was thus the predicted response magnitude had the subject attended for similar durations of times for all prior probability conditions. Even with this correction, responses to cued and uncued locations were qualitatively similar. Response magnitudes were similar for the 100 and 50% prior probability conditions for cued (0.30 vs. 0.29, 0.15 vs. 0.14, 0.24 vs. 0.17, 0.66 vs. 0.64, and 0.36 vs. 0.33% signal change with $P = 0.70$, 0.80, 0.12, 0.71, and 0.49 in V1-hV4 and V3A, respectively, uncorrected for multiple comparisons, paired *t*-test over subjects) and uncued locations (0.16 vs. 0.13, −0.05 vs. −0.10, −0.01 vs. −0.05, 0.45 vs. 0.47, and 0.16 vs. 0.21% signal change with $P = 0.27$, 0.06, 0.20, 0.57, and 0.06 in V1–4 and V3A, respectively, paired *t*-test; see above). On a subject-by-subject basis, only 12% of subject visual areas (3 of 25) had significantly larger responses for the 100 than 50% prior probability condition in the cued location, and only 32% of subject visual areas (8 of 25) showed significantly different responses for the uncued locations, but six of these showed, counterintuitively, less suppression for uncued locations as prior probability increased. As for cue sensitivity, the difference in response between cued and uncued locations did not differ significantly from 100 to 50% prior probability conditions ($P = 0.45$, 0.26, 0.43, 0.52, and 0.14 in V1–4 and V3A, respectively, paired *t*-test). On a subject-by subject basis, only 20% of subject visual areas (5 of 25) showed differences in cue sensitivity with prior probability, with three paradoxically showing greater cue sensitivity as prior probability was reduced. Thus, even if we accounted for the potential increase in underestimation of response magnitude with increasing prior probability, cortical responses still did not track changes in prior probability.

Efficient-selection model. Having found that BOLD responses did not strictly scale with prior probability in magnitude, cue sensitivity, or contrast sensitivity, we asked whether "efficient selection" (Pestilli et al. 2011) could account for graded behavioral performance that scaled with prior probability. Our model of efficient selection conceptualizes the neural process underlying contrast discrimination using a signal-detection (Green and Swets 1966) framework in which sensory signals for the four different grating stimuli are weighted by their magnitude and then pooled together so that perceptual decisions are made using pooled response distributions. Our model assesses how contrast-discrimination performance can improve due to enhancements in sensory representations, for example, by response enhancement (improvements in contrast sensitivity) and noise reduction, as well as changes in the efficiency with which relevant sensory signals for perceptual processing are selected.

How changes in sensory representation affect behavioral performance can be appreciated by examining how response magnitude and variability are estimated for the model. The model starts by estimating the response magnitude to each of the four stimuli (Fig. 4*A*) from a parameterized version (linear, with slope and intercept parameters) of the measured contrast-response functions (Fig. 4*B*). For each stimulus, the appropriately matching contrast-response function is used to estimate the response magnitude; for the example in Fig. 4, response magnitudes for the two cued locations (*top*) are estimated based on the contrast-response function for the 50% prior probability cued condition (solid blue lines), and the two uncued locations (*bottom*) are estimated from the contrast

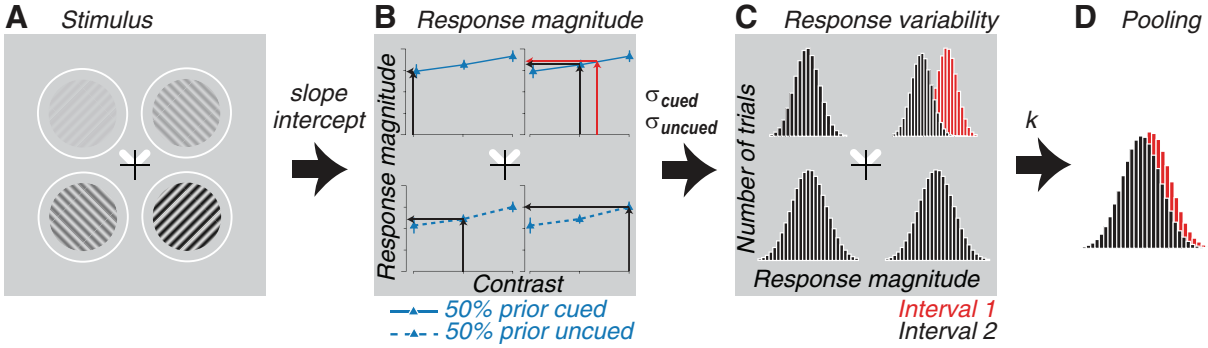

Fig. 4. Schematic diagram of the efficient-selection model. The response magnitude evoked by each contrast grating in the stimulus (*A*) is estimated from an interpolated contrast-response function measured with BOLD imaging (*B*). Note that the response magnitude for the 2 *top* cued locations are estimated from the contrast-response functions for cued locations (solid blue lines) and the 2 *bottom* uncued locations from the contrast-response functions for uncued locations (dashed blue lines) in the 50% prior probability condition. Only 1 of the locations (target, *top right* in this example) has a difference in contrast between the first (red) and second (black) intervals; for the rest of the locations, the response for the second (black) interval overlaps completely with the first (red, not visible due to overlap) interval. These response magnitudes are transformed into Gaussian response distributions (*C*) using the standard deviation (σ) parameter(s) of the model. In this example, the 2 *top* cued locations have a smaller σ then the lower uncued locations ($\sigma_{cued} < \sigma_{uncued}$). Again, note that the response distribution of the second (black) interval completely overlaps with the first (red, not visible) interval at nontarget locations. The 4 sets of response distributions are combined according to the pooling rule (*Eq. 2*) with parameter k. Discriminability is determined from the pooled distributions (*D*). Model parameters are indicated above each arrow in the diagram.

responses for the 50% prior probability uncued condition (dashed blue lines). Because cortical responses increase with contrast, the interval with the higher contrast can be discriminated as the one that evoked the larger response (Fig. 4*B*, red horizontal arrow is higher in response magnitude than the black horizontal arrow). Better performance can be achieved through increased contrast sensitivity, i.e., increasing the slope of the contrast-response function, which increases the difference in magnitude of responses to different contrasts. However, since our analysis of the contrast-response functions measured in the present study and previous published results (Buracas and Boynton 2007; Murray 2008; Pestilli et al. 2011) did not find any systematic difference in contrast sensitivity between cueing conditions, we fit a single slope to all contrast-response functions and only allowed the response offset (intercept) to change between conditions. Next, the response variability at each location was fit with a model parameter (σ) which could be different for cued and uncued locations, thus giving rise to response distributions of varying widths for each of the four stimuli (Fig. 4*C*). Noise reduction as has been reported in monkey physiology experiments can be achieved by decreased correlation between neurons for cued as opposed to uncued targets (Cohen and Maunsell 2009; Mitchell et al. 2009), which results in smaller response variability for cued locations when neural responses are averaged across populations [Fig. 4*C*, note the difference in width of example response distributions for the cued locations (*top*) as opposed to the uncued locations (*bottom*)].

How efficient selection can affect model behavioral performance can be appreciated by examining how the model pools sensory responses. Sensory response distributions (Fig. 4*C*) were pooled according to a rule (*Eq. 2*) whose parameter k determined whether they were simply averaged together ($k = 1$) or weighted according to the magnitude of response ($k > 1$). When $k > 1$, very large responses will pass through the pooling rule, whereas smaller responses will be suppressed. The larger the value of k, the closer the rule approximates max pooling, in which the largest response is the only response that passes through the pooling rule. Because cued locations evoke larger responses, $k > 1$ allows for cued responses to pass but suppresses the task-irrelevant, uncued responses, allowing efficient selection to improve discrimination performance. Note that this behavior does not require the pooling rule itself (setting of k) to change between cue conditions and is instead based on the measured relative difference in magnitude of evoked responses across locations under different cue conditions: if responses have similar magnitudes (for example, when all 4 locations are cued), they will be averaged together even if $k > 1$, and if responses have larger differences across locations (for example, when a single location is cued), the largest response will have a higher weighting. Behavioral performance of the model (d′) can be estimated from the pooled distributions (Fig. 4*D*) by computing the difference in the mean of the two distributions divided by the standard deviation.

We fit the model simultaneously to the measured cortical contrast-response functions and measured behavioral contrast-discrimination data and found that efficient selection could quantitatively account for improved behavioral performance with increasing prior probability of spatial cues. This version of the model tested the effects of efficient selection by allowing k to be fit to the data while not allowing for any noise reduction by forcing σ to be the same value for both cued and uncued locations (i.e., $\sigma_{cued} = \sigma_{uncued}$). This model fit well both the measured contrast-response functions (Fig. 5*A*, $r^2 = 0.77$) and behavioral performance (Fig. 5*B*, $r^2 = 0.86$) for V1. Fits were equally good for contrast-response function data from the other visual areas (contrast-response $r^2 = 0.79$, 0.85, 0.82, and 0.90, and contrast-discrimination $r^2 = 0.85$, 0.86, 0.87, and 0.88 for V2–4 and V3A, respectively). Of particular note, the efficient-selection model could account for three main features of the behavioral data (Fig. 5*B*): *1*) the difference in behavioral performance between the 100, 50, and 25% prior probability conditions (vertical offsets of the dark, medium, and light blue lines), *2*) the improvement in performance as a function of pedestal contrast (downward slopes of contrast-discrimination functions), and *3*) the decreasing effect of pedestal contrast on discrimination threshold as a function of cue condition [i.e., the downward slope of contrast-discrimination functions is most evident in the 25% prior probability condition (light blue line) and least evident in the 100% prior probability condition (dark

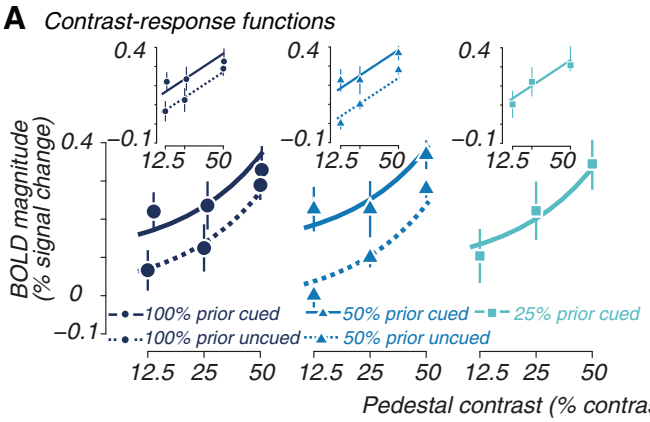

Fig. 5. Efficient selection provides good fits of cortical activity and behavioral performance. *A*: contrast-response functions are plotted on a semi-log axis in main panels and on a linear axis in *insets*. Solid and dashed lines are fit from the efficient-selection model, whereas data points are measured BOLD responses. *B*: main panel shows measured discrimination thresholds (data points) and model fits (solid lines) for efficient selection on a semi-log axis, and *inset* displays the same set of contrast-discrimination functions on a log-log axis.

blue line)]. The model's ability to fit the effect of pedestal contrast on the contrast-discrimination threshold (see *2* and *3* above) was due to the decreased effect of distractors when the target had a high pedestal contrast (in a given trial, each distractor had a pseudorandomized contrast of 12.5, 25, or 50% contrast and thus competed less with the target pedestal contrast when the target had high contrast than when it had low contrast; see Fig. 9 of Pestilli et al. 2011). These fits were achieved with k values that weighted larger responses more in the pooled response (k = 5.64, 4.65, 4.92, 4.97, and 4.81 for V1–4 and V3A, respectively). The noise variability (σ = 0.023, 0.033, 0.030, 0.026, and 0.017 for V1–4 and V3A, respectively) was similar to those estimated in previous experiments (Pestilli et al. 2011). Although the model was best fit when the complete set of behavioral data was used (Fig. 2*C*), a qualitatively similar set of results was obtained if we used simultaneously collected behavioral data (Fig. 2*A*), albeit with lower variance of the contrast-discrimination data accounted for (r^2 = 0.77, 0.46, 0.84, 0.78, and 0.80 for V1–4 and V3A, respectively).

Previous results (Pestilli et al. 2011) have shown that a realistic amount of noise reduction could not account for behavioral enhancement; in the present study we extend that finding to show that noise reduction cannot account for changes in prior probability at all without assuming some form of efficient selection. The intuition is based on consideration of how reduction of variability at cued locations (Cohen and Maunsell 2009; Mitchell et al. 2009) would affect pooled responses. For the 100% prior probability condition, a single location is cued (Fig. 6*A*, *left*; *top right* location is cued), resulting in reduced variability at that location (distributions are narrower). Pooling without efficient selection would lead to pooled responses with substantial variability from uncued locations (Fig. 6*A*, *right*; pooled distributions are wide). Paradoxically, cueing all four locations in the 25% prior probability condition would (Cohen and Maunsell 2009; if we simply extrapolate from findings that did not explicitly test such a condition, Mitchell et al. 2009) result in reduced variability at all locations (Fig. 6*B*, *left*) and, after pooling without efficient selection, reduced variability in the pooled responses (Fig. 6*B*, *right*). This reduced variability in the pooled responses would be expected to give better, not worse, performance as prior probability is reduced, contrary to what we found behaviorally. Therefore, if we try to fit the behavioral data without efficient selection, assuming noise reduction of about 50% for cued locations ($2\sigma_{cued} = \sigma_{uncued}$) to simulate results from the monkey physiology literature (Cohen and Maunsell 2009; Zohary et al. 1994), the model predicts the opposite of what we found behaviorally: improvements in behavioral performance (reduction in discrimination thresholds, Fig. 6*C*) with decreasing prior probability.

The efficient-selection model fits for the current data showed smaller exponents (k = 5.64 in V1; see above) compared with data from our previous study (k = 68.08; Pestilli et al. 2011), suggesting somewhat less efficient pooling and correspondingly poorer behavioral performance in the current data set. We next explored how significant this difference from the previous report was by asking how large a change in predicted behavioral performance would be expected for such changes in exponent magnitude. We used the efficient-selection model (σ constrained to be the same for cued and uncued locations) and systematically changed k and examined predicted contrast-discrimination thresholds. We found that as k increased from 1, there was a rapid increase in behavioral enhancement with cueing (Fig. 7). The threshold ratio between the 25 and 100% prior probability conditions (Fig. 7, light blue line), which measures how many times better performance is with 100 compared with 25% prior probability conditions, increased rapidly and saturated. The ratio between the 50 and 100% prior probability conditions showed a similar behavior and saturated at a lower ratio (Fig. 7, blue line). The dependence on k was similar for both the 25 and 50% prior probability threshold ratios, as can be seen in the *inset*, which displays the ratios normalized by their maximum value. Thus the values of k obtained in the current experiment results in better performance with prior probability, but higher values of k which fit previous experiments suggest that subjects in the previous experiment were performing modestly better, near-optimally given the model.

Efficient-selection model predictions for distractor effects. If a distractor is of high contrast, it will evoke a large response at a task-irrelevant location, and a prediction of the efficient-selection model is that it will substantially disrupt behavioral performance. Whereas this prediction was explicitly tested and validated in a previous work (Pestilli et al. 2011), we have extended those predictions to all of the prior probability conditions tested in the present work. In particular, as prior probability decreases, fewer locations will have large responses due to cueing, and so performance should be more disrupted by the presence of a high-contrast distractor. We

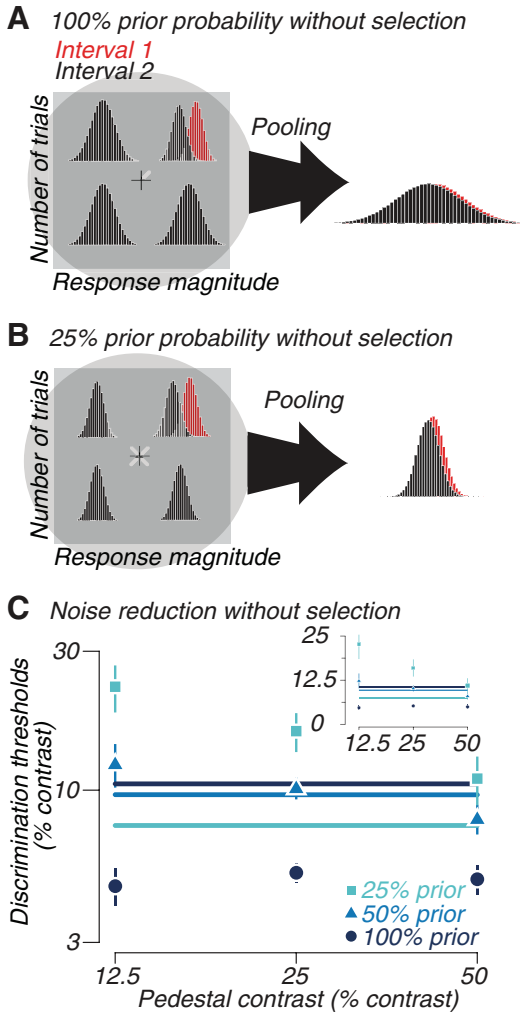

Fig. 6. Noise reduction without efficient selection predicts worse behavioral performance with increasing prior probability, opposite to observations. Schematic diagram show predictions of noise reduction without selective pooling for the 100 (*A*) and 25% (B) prior probability conditions (see RESULTS, *Efficient-selection model*, for details). *C*: according to model fits made by assuming a 50% reduction in noise with cueing, pooling of across all locations equally (without selection) results in predictions (lines) that are opposite to observed behavioral data (points). Model parameters follow the same conventions as Fig. 5*B*.

tested for this effect by examining contrast-discrimination thresholds for the targets with a mid-level contrast (25%) when there was a distractor with higher contrast (50%) or when there was no distractor with higher contrast; these conditions occurred randomly within the experiment. Computing discrimination thresholds separately for when there was a high-contrast distractor or not, we found that for all prior probabilities, discrimination thresholds were worse with a high-contrast distractor, which matches predictions by our model of efficient selection (average difference in discrimination thresholds across subjects: −1.5, −6.4, and −10.8% contrast for 100, 50, and 25% prior probability conditions, $P < 0.05$, paired *t*-test).

DISCUSSION

Using a contrast-discrimination task with multiple possible target locations, we have shown that parametrically increasing the spatial specificity of prior cues, and thereby the prior probability that a given location will contain the discrimination target, resulted in graded improvements in behavioral performance. However, BOLD magnitude was not strictly graded with prior probability (c.f. Basso and Wurtz 1997; Dorris and Munoz 1998). Whereas responses were weakest when all locations were cued, cueing one or two locations, and thus changing the prior probability from 100 to 50%, did not result in any significant change in cortical response or cue sensitivity (difference in cortical response between cued and uncued locations). Moreover, contrast sensitivity was also not graded with prior probability, suggesting that graded performance improvements were not due to improved sensory representation that would be expected by changing the slope of the relationship between contrast and response (response enhancement) (Boynton et al. 1999; Foley and Legge 1981; Legge and Foley 1980; Nachmias and Sansbury 1974; Pestilli et al. 2011; Zenger-Landolt and Heeger 2003). Instead, we found that a model which links cortical responses to behavioral performance (Pestilli et al. 2011) could quantitatively account for graded performance enhancement by an efficient-selection mechanism in which the magnitude of sensory responses weighs how sensory evidence from different locations are pooled together to form perceptual decisions.

Versatile allocation of spatial attention. Our results support the notion that the human ability to allocate spatial attention according to the relevance of locations is versatile. Behavior in our task was consistent with both a single attentional focus (Posner et al. 1980) that can be adjusted like a zoom lens (Eriksen and St James 1986) and split, multiple attentional foci (Awh and Pashler 2000; Castiello and Umiltá 1992). Splitting attention has been demonstrated with the use of physiological measurements (McMains and Somers 2004; Morawetz et al. 2007; Müller et al. 2003a) and has been suggested to incur little processing overhead (McMains and Somers 2005). Splitting of attention is advantageous when there are intervening stimuli between locations of relevance, which was not the case for our task. Other models of attention suggest that subjects may switch attention from one location to another (Sperling and

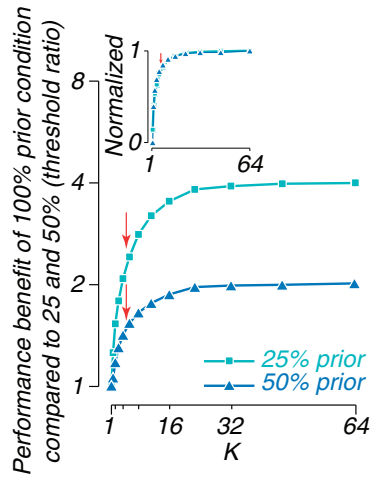

Fig. 7. Model predictions for behavioral performance improve rapidly with increasing exponent *k*. *A* shows plots of the discrimination thresholds of the 25 and 50% prior probability conditions divided by the 100% prior probability condition, a measure of how many times better performance becomes in the 100% prior probability condition compared with the lower prior probability conditions. Red arrows mark the value of *k* estimated by the efficient-selection model. *Inset* shows the same 2 curves normalized to the same maximum value.

Melchner 1978). This model is unlikely, since it predicts that the average attentional modulation when attending to two locations would be roughly half of that found when attending to a single location, in contradiction to our results. According to the normalization model of attention (Reynolds and Heeger 2009), versatility of spatial attention allocation can account for various different types of modulations of contrast response for single units (Lee and Maunsell 2010; Martínez-Trujillo and Treue 2002; Pooresmaeili et al. 2010; Reynolds et al. 2000; Thiele et al. 2009; Williford and Maunsell 2006), which when averaged across large populations, as BOLD measurements implicitly do, may appear as additive offsets (Hara et al. 2014) as measured in the present study.

Sensory enhancement or efficient selection. In our analysis, efficient selection rather than sensory enhancement accounted for graded behavioral performance with prior probability, but this does not imply that attention always acts primarily through improved selection, gating (Fischer and Whitney 2012), or synaptic transmission (Briggs et al. 2013) of sensory signals. We did not find any evidence for sensory enhancement in the form of improved contrast sensitivity (i.e., increased slope of contrast-response), nor did modeled noise reduction without selection improve behavioral performance, so instead we concluded that efficient selection plays a dominant role in gradually enhancing behavioral performance with prior probability. Efficient selection may be particularly important when a visual scene is cluttered (c.f. Ciaramitaro et al. 2001; Pestilli and Carrasco 2005); tasks which involve multiple targets like ours are more likely to benefit from improved selection than tasks which involve only one or two targets. Moreover, the particular task performed may influence whether sensory enhancement or efficient selection plays a dominant role. In orientation discrimination, for example, neurons whose orientation tuning provides the most amount of information relevant to discrimination may already be more strongly weighted than others (Jazayeri and Movshon 2007; Purushothaman and Bradley 2005; Scolari and Serences 2009, 2010; Scolari et al. 2012; Seung and Sompolinsky 1993; Verghese et al. 2012) so that additional selection through attentional selection may be less effective. Indeed, sensory enhancement in the form of sharpened orientation tuning has been reported for orientation discrimination when prior information is provided in humans (Anderson et al. 2013; Jehee et al. 2011; Kok et al. 2012), though not in monkeys (McAdams and Maunsell 1999). Contrast discrimination may benefit more from summation across many neurons all with monotonically increasing contrast responses (Verghese et al. 2012), and therefore behavioral performance may tend to be initially based on a less selective sampling of neurons. Efficient selection then, particularly in the presence of multiple possible targets, may be a more critical neural mechanism for improving behavioral performance.

Hemodynamic coupling to neural activity. The exact link between neural and hemodynamic activity is an area of active research (Logothetis 2008), leading to uncertainty in the interpretation of BOLD activity with attention (for a discussion relevant to the tasks studied here, see Pestilli et al. 2011). In some cases hemodynamic activity appears better correlated with perception than spiking activity (Boynton 2011; Maier et al. 2008). Hemodynamic activity without corresponding spiking activity has been reported (Sirotin and Das 2009), raising the possibility that attentional modulations of hemodynamic response are unrelated to changes in neural activity. However, combined blood flow and oxygenation measurements suggest that attention in humans incurs a substantially increased cerebral metabolic rate of oxygen consumption (Moradi et al. 2012). Thus BOLD responses may be sensitive to small changes in neural activity with attention summed across many neurons (Luck et al. 1997). Importantly, voltage-sensitive dye (VSD) measurements of monkey V1 during a comparable task to ours found attentional modulations that were indistinguishable whether one or four locations were being cued (Chen and Seidemann 2012), thus supporting a similar conclusion to ours about the importance of gating or efficient selection rather than sensory enhancement. Thus VSD measurements and other evidence support our conclusion that neural responses are not scaled with prior probability and suggest that considerations of spatial scale of measurements, rather than differences related to the origin of BOLD signals, can explain some apparent discrepancies between single-unit and BOLD measurements (Boynton 2011). Nonetheless, there are caveats. VSD measurements do not distinguish excitatory and inhibitory responses, which could lead to discrepancies between gross VSD measurements and the responses due to excitatory population activity if the typical balance (Haider et al. 2006; Isaacson and Scanziani 2011; Mariño et al. 2005; Shadlen and Newsome 1998) between excitatory and inhibitory signals is altered by attention state (Haider et al. 2012; Zhou et al. 2014). Moreover, attention states may recruit neuromodulatory signals (Yu and Dayan 2005) that could change the relationship between BOLD and spiking activity in ways that are not yet known.

The efficient-selection model was built on the assumption of a linear relationship between BOLD responses and neural firing, i.e., that increases in spiking with stimulus contrast is associated with a proportional change in the BOLD response. Experiments which have directly examined hemodynamic measures compared with neural firing rates as a function of stimulus contrast have predominantly supported this linear assumption. Direct comparison of multi-unit and local field potential (LFP) measures with concurrently measured BOLD responses for contrast response shows a relationship that is approximately linear with a non-zero intercept (Fig. 5 of Logothetis et al. 2001), and comparison of BOLD responses and measured single-unit contrast response across species shows strong linear agreement (Heeger et al. 2000). Concurrent measurement of optical imaging with intrinsic signals and measurements of spiking of individual neurons have shown that after removal of a nonspecific signal (Sirotin and Das 2009) by subtraction, the relationship between hemodynamic response and spiking response is linear (Fig. 3*C* of Cardoso et al. 2012). The subtraction procedure applied to our data did not substantially change our results.

Nonetheless, there is a diversity of experimental evidence regarding the relationship of hemodynamic to electrophysiological responses; as long as the relationship is linear or compressive, the conclusions of our modeling would not qualitatively change. That is, a compressive relationship suggests that at high baseline BOLD activity, differences in BOLD responses would signal smaller differences in electrophysiological signals than at low baseline BOLD activity. Because we have found that at high prior probability, cued targets have a higher baseline BOLD activity, this would suggest that the

measured differences in response for different contrasts would correspond to smaller, less discriminable differences in electrophysiological activity. This contradicts a sensory enhancement account in which attention acts to improve the discriminability of sensory signals. Compressive (or, equivalently, expansive if reported as the dependence of hemodynamic activity on electrophysiological activity) (Devor et al. 2003; Li and Freeman 2007; Offenhauser et al. 2005; Sheth et al. 2004), linear (Arthurs et al. 2000; Ogawa et al. 2000; Ngai et al. 1999; Smith et al. 2002). and threshold-linear relationships (Logothetis et al. 2001; Nemoto et al. 2004; Schummers et al. 2008) have been reported between optical measurements of hemodynamic activity and electrophysiology in numerous experiments. Moreover, the relationship between BOLD responses and estimated metabolic rate of oxygen consumption has been reported to be compressive (Liang et al. 2013), supporting similar conclusions. Conversely, a sigmoidal (Norup Nielsen and Lauritzen 2001) or inverse-sigmoidal relationship (Jones et al. 2004) between hemodynamic and electrophysiological signals would be able to predict behavioral performance enhancement without efficient selection for the range of hemodynamic response levels in which the relationship is compressive. The totality of the evidence therefore suggests a relationship between hemodynamic and spiking measures, which is compatible with our conclusion that efficient selection can account for graded changes in behavioral performance.

Limited resources. That behavioral improvements are graded with spatial specificity of prior cues suggests that a limited resource is being distributed to handle the processing of cued stimuli. However, our data provide little support for this limited resource being observable in early visual cortex activity. No significant difference in response between the 100 and 50% prior probability conditions was observed. There was a small overall decrease in response for the 25% prior probability condition when all four locations were cued (Müller et al. 2003b; c.f. McMains and Somers 2004). However, cueing all items is a special case where attention is spread across the whole visual field and experimentally prohibits evaluation of the difference in response between cued and uncued stimuli. Particularly for decision models that compare the responses for multiple different stimuli as our efficient-selection model does, the relative difference between response magnitudes for the different stimuli is more important than the difference in response magnitude relative to an arbitrary gray-screen baseline.

If attentional modulation between cued and uncued locations is not resource limited in early visual cortex, what does limit performance? Noise reduction is a possibility. Electrophysiological studies suggest that intrinsic variability and correlations in neural firing decrease with attention in V4 (Cohen and Maunsell 2009; Mitchell et al. 2009). This could account for behavioral enhancement, particularly in tasks with few stimuli where behavior is limited by the sensitivity of sensory responses rather than the exclusion of external noise (Dosher and Lu 2000; Lu and Dosher 1998). However, our analysis showed that as more locations were cued, noise reduction of responses at different locations resulted in less noise after pooling, thus predicting better perception as more locations are cued, opposite to our observations. One explanation for decreased correlation with attention is that shared variability comes from a common source of inhibition which is suppressed at cued locations (Cohen and Maunsell 2009). If this is the case, why might neural circuits be constructed to inject shared variability and thereby reduce sensitivity? Perhaps decreased correlation is a side effect of inhibitory signals whose purpose is to control the overall magnitude of responses, which, according to our efficient-selection model, is what determines whether task-relevant signals can be distinguished from task-irrelevant signals.

Behavioral performance may also be limited by access to higher cognitive resources such as working memory or perceptual processes. Our efficient-selection model leaves open the question of what resource the selection process controls access to. A simple possibility is that higher cortical areas receive pooled sensory signals which have undergone efficient selection so that performance is limited by the degrading effects of representing information from distractor locations as well as task-relevant target locations. Another possibility is that working memory limits performance while efficient selection controls which sensory responses are encoded in working memory (Cowan et al. 2005; Uncapher and Rugg 2009; Vogel et al. 2005). We intentionally kept the working memory load low in our task by limiting the number of discrete targets (Cowan 2001; Fukuda et al. 2010; Luck and Vogel 1997; Miller 1956) and the duration of the interstimulus interval. Nonetheless, access to working memory can affect task performance (Vogel et al. 2005), and the role of efficient selection may be to ensure that the correct visual stimuli are stored in working memory.

Our task shares several features of classical search paradigms (Eckstein 2011) but differs in several respects. First, there are a fixed number of stimuli, making interpretation easier than examining increases in set size, which can covary with stimulus density and increases in sensory interactions. Second, the target location is specified at the end of the trial, reducing uncertainty (Pelli 1985) about target location during the response interval. Finally, our manipulation increased the number of monitored locations, not the set size in which an object must be searched. Nonetheless, conceptual views of the processes that limit search performance may be relevant.

In particular, a statistical decision-making framework (Palmer et al. 2000; Verghese 2001), in which performance gets worse with increasing number of objects because noisy distractor responses become more likely to exceed the decision threshold for target presence, has been used to explain search performance. Refinement of this view suggests that an optimal Bayesian observer could improve performance by weighing the sensory evidence from each possible object location according to both the quality (Ma et al. 2011) and the prior probability that the location contains the target (Eckstein 2011; Shaw 1984; Shaw and Shaw 1977). When applied to our task, this suggests that observers should weight sensory evidence according to the probability that each location contains the target, the prior probability. Indeed, we see graded enhancements in performance which roughly track prior probability. While our BOLD measurements did not find a one-to-one correspondence between response magnitude and prior probability, response increases, when fed through the efficient-selection mechanism, did predict the observed graded behavioral results. Thus our results suggest that rather than explicitly encoding prior probability in early visual cortex, efficient selection, as implemented by the weighting of sensory responses according to their magnitude, can pool responses appropriately as long as

each probable, task-relevant location induces similarly large responses compared with task-irrelevant locations.

ACKNOWLEDGMENTS

We thank Kenji Haruhana and the Support Unit for Functional Magnetic Resonance Imaging at RIKEN Brain Science Institute for assistance in conducting experiments. We also thank Toshiko Ikari for administrative support and Arman Abrahamyan, Andrew Meso, and Franco Pestilli for comments on an earlier version of this manuscript.

Present address for J. L. Gardner: Department of Psychology, Stanford University, Stanford, CA 94305.

GRANTS

This work was supported in part by Grants-in-Aid for Scientific Research 24300146 (to J. L. Gardner) from the Japanese Ministry of Education, Culture, Sports, Science and Technology (MEXT).

DISCLOSURES

No conflicts of interest, financial or otherwise, are declared by the authors.

AUTHOR CONTRIBUTIONS

Y.H. and J.L.G. conception and design of research; Y.H. and J.L.G. performed experiments; Y.H. and J.L.G. analyzed data; Y.H. and J.L.G. interpreted results of experiments; Y.H. and J.L.G. prepared figures; Y.H. and J.L.G. drafted manuscript; Y.H. and J.L.G. edited and revised manuscript; J.L.G. approved final version of manuscript.

REFERENCES

Abrams J, Nizam A, Carrasco M. Isoeccentric locations are not equivalent: the extent of the vertical meridian asymmetry. *Vision Res* 52: 70–78, 2012.

Albrecht DG, Hamilton DB. Striate cortex of monkey and cat: contrast response function. *J Neurophysiol* 48: 217–237, 1982.

Alvarez GA, Cavanagh P. Independent resources for attentional tracking in the left and right visual hemifields. *Psychol Sci* 16: 637–643, 2005.

Alvarez GA, Gill J, Cavanagh P. Anatomical constraints on attention: hemifield independence is a signature of multifocal spatial selection. *J Vis* 12: 9, 2012.

Anderson DE, Ester EF, Serences JT, Awh E. Attending multiple items decreases the selectivity of population responses in human primary visual cortex. *J Neurosci* 33: 9273–9282, 2013.

Arthurs OJ, Williams EJ, Carpenter TA, Pickard JD, Boniface SJ. Linear coupling between functional magnetic resonance imaging and evoked potential amplitude in human somatosensory cortex. *Neuroscience* 101: 803–806, 2000.

Awh E, Pashler H. Evidence for split attentional foci. *J Exp Psychol Hum Percept Perform* 26: 834–846, 2000.

Basso MA, Wurtz RH. Modulation of neuronal activity by target uncertainty. *Nature* 389: 66–69, 1997.

Boynton GM. Spikes, BOLD, attention, and awareness: a comparison of electrophysiological and fMRI signals in V1. *J Vis* 11: 12, 2011.

Boynton GM, Demb JB, Glover GH, Heeger DJ. Neuronal basis of contrast discrimination. *Vision Res* 39: 257–269, 1999.

Boynton GM, Engel SA, Glover GH, Heeger DJ. Linear systems analysis of functional magnetic resonance imaging in human V1. *J Neurosci* 16: 4207–4221, 1996.

Briggs F, Mangun GR, Usrey WM. Attention enhances synaptic efficacy and the signal-to-noise ratio in neural circuits. *Nature* 499: 476–480, 2013.

Buracas GT, Boynton GM. The effect of spatial attention on contrast response functions in human visual cortex. *J Neurosci* 27: 93–97, 2007.

Cardoso MM, Sirotin YB, Lima B, Glushenkova E, Das A. The neuroimaging signal is a linear sum of neurally distinct stimulus- and task-related components. *Nat Neurosci* 15: 1298–1306, 2012.

Carrasco M. Visual attention: the past 25 years. *Vision Res* 51: 1484–1525, 2011.

Castiello U, Umiltá C. Splitting focal attention. *J Exp Psychol Hum Percept Perform* 18: 837–848, 1992.

Chen Y, Seidemann E. Attentional modulations related to spatial gating but not to allocation of limited resources in primate V1. *Neuron* 74: 557–566, 2012.

Ciaramitaro VM, Cameron EL, Glimcher PW. Stimulus probability directs spatial attention: an enhancement of sensitivity in humans and monkeys. *Vision Res* 41: 57–75, 2001.

Cohen MR, Maunsell JH. Attention improves performance primarily by reducing interneuronal correlations. *Nat Neurosci* 12: 1594–1600, 2009.

Cowan N. The magical number 4 in short-term memory: a reconsideration of mental storage capacity. *Behav Brain Sci* 24: 87–114, 2001.

Cowan N, Elliott EM, Scott Saults J, Morey CC, Mattox S, Hismjatullina A, Conway ARA. On the capacity of attention: its estimation and its role in working memory and cognitive aptitudes. *Cogn Psychol* 51: 42–100, 2005.

Dale AM, Fischl B, Sereno MI. Cortical surface-based analysis. I. Segmentation and surface reconstruction. *Neuroimage* 9: 179–194, 1999.

Desimone R, Duncan J. Neural mechanisms of selective visual attention. *Annu Rev Neurosci* 18: 193–222, 1995.

Devor A, Dunn AK, Andermann ML, Ulbert I, Boas DA, Dale AM. Coupling of total hemoglobin concentration, oxygenation, and neural activity in rat somatosensory cortex. *Neuron* 39: 353–359, 2003.

Dhruv NT, Carandini M. Cascaded effects of spatial adaptation in the early visual system. *Neuron* 81: 529–535, 2014.

Dhruv NT, Tailby C, Sokol SH, Lennie P. Multiple adaptable mechanisms early in the primate visual pathway. *J Neurosci* 31: 15016–15025, 2011.

Dorris MC, Munoz DP. Saccadic probability influences motor preparation signals and time to saccadic initiation. *J Neurosci* 18: 7015–7026, 1998.

Dosher BA, Lu ZL. Mechanisms of perceptual attention in precuing of location. *Vision Res* 40: 1269–1292, 2000.

Eckstein MP. Visual search: a retrospective. *J Vis* 11: 14, 2011.

Eckstein MP, Peterson MF, Pham BT, Droll JA. Statistical decision theory to relate neurons to behavior in the study of covert visual attention. *Vision Res* 49: 1097–1128, 2009.

Eriksen CW, St James JD. Visual attention within and around the field of focal attention: a zoom lens model. *Percept Psychophys* 40: 225–240, 1986.

Fischer J, Whitney D. Attention gates visual coding in the human pulvinar. *Nat Commun* 3: 1051, 2012.

Foley JM, Legge GE. Contrast detection and near-threshold discrimination in human vision. *Vision Res* 21: 1041–1053, 1981.

Fukuda K, Awh E, Vogel EK. Discrete capacity limits in visual working memory. *Curr Opin Neurobiol* 20: 177–182, 2010.

Gardner JL, Merriam EP, Movshon JA, Heeger DJ. Maps of visual space in human occipital cortex are retinotopic, not spatiotopic. *J Neurosci* 28: 3988–3999, 2008.

Gardner JL, Sun P, Waggoner RA, Ueno K, Tanaka K, Cheng K. Contrast adaptation and representation in human early visual cortex. *Neuron* 47: 607–620, 2005.

Green DM, Swets JA. *Signal Detection Theory and Psychophysics*. New York: Wiley, 1966.

Haider B, Duque A, Hasenstaub AR, McCormick DA. Neocortical network activity in vivo is generated through a dynamic balance of excitation and inhibition. *J Neurosci* 26: 4535–4545, 2006.

Haider B, Häusser M, Carandini M. Inhibition dominates sensory responses in the awake cortex. *Nature* 493: 97–100, 2012.

Hara Y, Pestilli F, Gardner JL. Differing effects of attention in single-units and populations are well predicted by heterogeneous tuning and the normalization model of attention. *Front Comput Neurosci* 8: 12, 2014.

He S, Cavanagh P, Intriligator J. Attentional resolution and the locus of visual awareness. *Nature* 383: 334–337, 1996.

Heeger DJ, Huk AC, Geisler WS, Albrecht DG. Spikes versus BOLD: what does neuroimaging tell us about neuronal activity? *Nat Neurosci* 3: 631–632, 2000.

Hu X, Le TH, Parrish T, Erhard P. Retrospective estimation and correction of physiological fluctuation in functional MRI. *Magn Reson Med* 34: 201–212, 1995.

Isaacson JS, Scanziani M. How inhibition shapes cortical activity. *Neuron* 72: 231–243, 2011.

Itti L, Koch C. Computational modelling of visual attention. *Nat Rev Neurosci* 2: 194–203, 2001.

Jazayeri M, Movshon JA. A new perceptual illusion reveals mechanisms of sensory decoding. *Nature* 446: 912–915, 2007.

Jehee JFM, Brady DK, Tong F. Attention improves encoding of task-relevant features in the human visual cortex. *J Neurosci* 31: 8210–8219, 2011.

Jones M, Hewson-Stoate N, Martindale J, Redgrave P, Mayhew J. Nonlinear coupling of neural activity and CBF in rodent barrel cortex. *Neuroimage* 22: 956–965, 2004.

Kastner S, Ungerleider LG. Mechanisms of visual attention in the human cortex. *Annu Rev Neurosci* 23: 315–341, 2000.

Kiani R, Hanks TD, Shadlen MN. Bounded integration in parietal cortex underlies decisions even when viewing duration is dictated by the environment. *J Neurosci* 28: 3017–3029, 2008.

Kohn A. Visual adaptation: physiology, mechanisms, and functional benefits. *J Neurophysiol* 97: 3155–3164, 2007.

Kok P, Jehee JFM, de Lange FP. Less is more: expectation sharpens representations in the primary visual cortex. *Neuron* 75: 265–270, 2012.

Kontsevich LL, Tyler CW. Bayesian adaptive estimation of psychometric slope and threshold. *Vision Res* 39: 2729–2737, 1999.

Lee DK, Itti L, Koch C, Braun J. Attention activates winner-take-all competition among visual filters. *Nat Neurosci* 2: 375–381, 1999.

Lee J, Maunsell JHR. The effect of attention on neuronal responses to high and low contrast stimuli. *J Neurophysiol* 104: 960–971, 2010.

Legge GE, Foley JM. Contrast masking in human vision. *J Opt Soc Am A* 70: 1458–1471, 1980.

Levitt H. Transformed up-down methods in psychoacoustics. *J Acoust Soc Am* 49, *Suppl* 2: 467, 1971.

Li B, Freeman RD. High-resolution neurometabolic coupling in the lateral geniculate nucleus. *J Neurosci* 27: 10223–10229, 2007.

Li X, Lu ZL, Tjan BS, Dosher BA, Chu W. Blood oxygenation level-dependent contrast response functions identify mechanisms of covert attention in early visual areas. *Proc Natl Acad Sci USA* 105: 6202–6207, 2008.

Liang CL, Ances BM, Perthen JE, Moradi F, Liau J, Buracas GT, Hopkins SR, Buxton RB. Luminance contrast of a visual stimulus modulates the BOLD response more than the cerebral blood flow response in the human brain. *Neuroimage* 64: 104–111, 2013.

Logothetis NK. What we can do and what we cannot do with fMRI. *Nature* 453: 869–878, 2008.

Logothetis NK, Pauls J, Augath M, Trinath T, Oeltermann A. Neurophysiological investigation of the basis of the fMRI signal. *Nature* 412: 150–157, 2001.

Lu ZL, Dosher BA. External noise distinguishes attention mechanisms. *Vision Res* 38: 1183–1198, 1998.

Luck SJ, Chelazzi L, Hillyard SA, Desimone R. Neural mechanisms of spatial selective attention in areas V1, V2, and V4 of macaque visual cortex. *J Neurophysiol* 77: 24–42, 1997.

Luck SJ, Vogel EK. The capacity of visual working memory for features and conjunctions. *Nature* 390: 279–281, 1997.

Ma WJ, Navalpakkam V, Beck JM, Berg RV, Pouget A. Behavior and neural basis of near-optimal visual search. *Nat Neurosci* 14: 783–790, 2011.

Maier A, Wilke M, Aura C, Zhu C, Ye FQ, Leopold DA. Divergence of fMRI and neural signals in V1 during perceptual suppression in the awake monkey. *Nat Neurosci* 11: 1193–1200, 2008.

Mariño J, Schummers J, Lyon DC, Schwabe L, Beck O, Wiesing P, Obermayer K, Sur M. Invariant computations in local cortical networks with balanced excitation and inhibition. *Nat Neurosci* 8: 194–201, 2005.

Martínez-Trujillo J, Treue S. Attentional modulation strength in cortical area MT depends on stimulus contrast. *Neuron* 35: 365–370, 2002.

McAdams CJ, Maunsell JH. Effects of attention on orientation-tuning functions of single neurons in macaque cortical area V4. *J Neurosci* 19: 431–441, 1999.

McMains SA, Somers DC. Multiple spotlights of attentional selection in human visual cortex. *Neuron* 42: 677–686, 2004.

McMains SA, Somers DC. Processing efficiency of divided spatial attention mechanisms in human visual cortex. *J Neurosci* 25: 9444–9448, 2005.

Miller GA. The magical number seven plus or minus two: some limits on our capacity for processing information. *Psychol Rev* 63: 81–97, 1956.

Mitchell JF, Sundberg KA, Reynolds JH. Spatial attention decorrelates intrinsic activity fluctuations in macaque area V4. *Neuron* 63: 879–888, 2009.

Moradi F, Buracas GT, Buxton RB. Attention strongly increases oxygen metabolic response to stimulus in primary visual cortex. *Neuroimage* 59: 601–607, 2012.

Morawetz C, Holz P, Baudewig J, Treue S, Dechent P. Split of attentional resources in human visual cortex. *Vis Neurosci* 24: 817–826, 2007.

Morrone MC, Denti V, Spinelli D. Color and luminance contrasts attract independent attention. *Curr Biol* 12: 1134–1137, 2002.

Murray SO. The effects of spatial attention in early human visual cortex are stimulus independent. *J Vis* 8: 2.1–11, 2008.

Müller JR, Metha AB, Krauskopf J, Lennie P. Rapid adaptation in visual cortex to the structure of images. *Science* 285: 1405–1408, 1999.

Müller MM, Malinowski P, Gruber T, Hillyard SA. Sustained division of the attentional spotlight. *Nature* 424: 309–312, 2003a.

Müller NG, Bartelt OA, Donner TH, Villringer A, Brandt SA. A physiological correlate of the "Zoom Lens" of visual attention. *J Neurosci* 23: 3561–3565, 2003b.

Nachmias J, Sansbury RV. Letter: Grating contrast: discrimination may be better than detection. *Vision Res* 14: 1039–1042, 1974.

Nemoto M, Sheth S, Guiou M, Pouratian N, Chen JWY, Toga AW. Functional signal- and paradigm-dependent linear relationships between synaptic activity and hemodynamic responses in rat somatosensory cortex. *J Neurosci* 24: 3850–3861, 2004.

Nestares O, Heeger DJ. Robust multiresolution alignment of MRI brain volumes. *Magn Reson Med* 43: 705–715, 2000.

Ngai AC, Jolley MA, D'Ambrosio R, Meno JR, Winn HR. Frequency-dependent changes in cerebral blood flow and evoked potentials during somatosensory stimulation in the rat. *Brain Res* 837: 221–228, 1999.

Norup Nielsen A, Lauritzen M. Coupling and uncoupling of activity-dependent increases of neuronal activity and blood flow in rat somatosensory cortex. *J Physiol* 533: 773–785, 2001.

Offenhauser N, Thomsen K, Caesar K, Lauritzen M. Activity-induced tissue oxygenation changes in rat cerebellar cortex: interplay of postsynaptic activation and blood flow. *J Physiol* 565: 279–294, 2005.

Ogawa S, Lee TM, Kay AR, Tank DW. Brain magnetic resonance imaging with contrast dependent on blood oxygenation. *Proc Natl Acad Sci USA* 87: 9868–9872, 1990.

Ogawa S, Lee TM, Stepnoski R, Chen W, Zhu XH, Ugurbil K. An approach to probe some neural systems interaction by functional MRI at neural time scale down to milliseconds. *Proc Natl Acad Sci USA* 97: 11026–11031, 2000.

Ohzawa I, Sclar G, Freeman RD. Contrast gain control in the cat visual cortex. *Nature* 298: 266–268, 1982.

Palmer J, Verghese P, Pavel M. The psychophysics of visual search. *Vision Res* 40: 1227–1268, 2000.

Pashler HE. *The Psychology of Attention*. Cambridge, MA: MIT Press, 1998.

Pelli DG. Uncertainty explains many aspects of visual contrast detection and discrimination. *J Opt Soc Am A* 2: 1508–1532, 1985.

Pestilli F, Carrasco M. Attention enhances contrast sensitivity at cued and impairs it at uncued locations. *Vision Res* 45: 1867–1875, 2005.

Pestilli F, Carrasco M, Heeger DJ, Gardner JL. Attentional enhancement via selection and pooling of early sensory responses in human visual cortex. *Neuron* 72: 832–846, 2011.

Pooresmaeili A, Poort J, Thiele A, Roelfsema PR. Separable codes for attention and luminance contrast in the primary visual cortex. *J Neurosci* 30: 12701–12711, 2010.

Posner MI, Snyder CR, Davidson BJ. Attention and the detection of signals. *J Exp Psychol* 109: 160–174, 1980.

Pruessmann KP, Weiger M, Scheidegger MB, Boesiger P. SENSE: sensitivity encoding for fast MRI. *Magn Reson Med* 42: 952–962, 1999.

Purushothaman G, Bradley DC. Neural population code for fine perceptual decisions in area MT. *Nat Neurosci* 8: 99–106, 2005.

Reynolds JH, Heeger DJ. The normalization model of attention. *Neuron* 61: 168–185, 2009.

Reynolds JH, Pasternak T, Desimone R. Attention increases sensitivity of V4 neurons. *Neuron* 26: 703–714, 2000.

Schummers J, Yu H, Sur M. Tuned responses of astrocytes and their influence on hemodynamic signals in the visual cortex. *Science* 320: 1638–1643, 2008.

Sclar G, Maunsell JH, Lennie P. Coding of image contrast in central visual pathways of the macaque monkey. *Vision Res* 30: 1–10, 1990.

Scolari M, Byers A, Serences JT. Optimal deployment of attentional gain during fine discriminations. *J Neurosci* 32: 7723–7733, 2012.

Scolari M, Serences JT. Adaptive allocation of attentional gain. *J Neurosci* 29: 11933–11942, 2009.

Scolari M, Serences JT. Basing perceptual decisions on the most informative sensory neurons. *J Neurophysiol* 104: 2266–2273, 2010.

Sergent C, Ruff CC, Barbot A, Driver J, Rees G. Top-down modulation of human early visual cortex after stimulus offset supports successful postcued report. *J Cogn Neurosci* 23: 1921–1934, 2011.

Seung HS, Sompolinsky H. Simple models for reading neuronal population codes. *Proc Natl Acad Sci USA* 90: 10749–10753, 1993.

Shadlen MN, Newsome WT. The variable discharge of cortical neurons: implications for connectivity, computation, and information coding. *J Neurosci* 18: 3870–3896, 1998.

Shaw ML. Division of attention among spatial locations-a fundamental difference between detection of letters and detection of luminance increments. In: *Attention and Performance X*, edited by Bouma H, Bouwhuis DG. Hillsdale, NJ: Erlbaum, 1984, p. 109–121.

Shaw ML, Shaw P. Optimal allocation of cognitive resources to spatial locations. *J Exp Psychol Hum Percept Perform* 3: 201–211, 1977.

Sheth SA, Nemoto M, Guiou M, Walker M, Pouratian N, Toga AW. Linear and nonlinear relationships between neuronal activity, oxygen metabolism, and hemodynamic responses. *Neuron* 42: 347–355, 2004.

Sirotin YB, Das A. Anticipatory haemodynamic signals in sensory cortex not predicted by local neuronal activity. *Nature* 457: 475–479, 2009.

Smith AJ, Blumenfeld H, Behar KL, Rothman DL, Shulman RG, Hyder F. Cerebral energetics and spiking frequency: the neurophysiological basis of fMRI. *Proc Natl Acad Sci USA* 99: 10765–10770, 2002.

Sperling G, Melchner MJ. The attention operating characteristic: examples from visual search. *Science* 202: 315–318, 1978.

Thiele A, Pooresmaeili A, Delicato LS, Herrero JL, Roelfsema PR. Additive effects of attention and stimulus contrast in primary visual cortex. *Cereb Cortex* 19: 2970–2981, 2009.

Tolhurst DJ, Movshon JA, Thompson ID. The dependence of response amplitude and variance of cat visual cortical neurones on stimulus contrast. *Exp Brain Res* 41: 414–419, 1981.

Tootell RB, Reppas JB, Kwong KK, Malach R, Born RT, Brady TJ, Rosen BR, Belliveau JW. Functional analysis of human MT and related visual cortical areas using magnetic resonance imaging. *J Neurosci* 15: 3215–3230, 1995.

Uncapher MR, Rugg MD. Selecting for memory? The influence of selective attention on the mnemonic binding of contextual information. *J Neurosci* 29: 8270–8279, 2009.

Van De Moortele PF, Auerbach EJ, Olman C, Yacoub E, Ugurbil K, Moeller S. T1 weighted brain images at 7 Tesla unbiased for proton density, T2* contrast and RF coil receive B1 sensitivity with simultaneous vessel visualization. *Neuroimage* 46: 432–446, 2009.

Verghese P. Visual search and attention: a signal detection theory approach. *Neuron* 31: 523–535, 2001.

Verghese P, Kim YJ, Wade AR. Attention selects informative neural populations in human V1. *J Neurosci* 32: 16379–16390, 2012.

Vogel EK, Mccollough AW, Machizawa MG. Neural measures reveal individual differences in controlling access to working memory. *Nature* 438: 500–503, 2005.

Wandell BA, Dumoulin SO, Brewer AA. Visual field maps in human cortex. *Neuron* 56: 366–383, 2007.

Weibull W. A statistical distribution function of wide applicability. *J Appl Mech* 18: 293–297, 1951.

Wichmann FA, Hill NJ. The psychometric function: I. Fitting, sampling, and goodness of fit. *Percept Psychophys* 63: 1293–1313, 2001.

Williford T, Maunsell JH. Effects of spatial attention on contrast response functions in macaque area V4. *J Neurophysiol* 96: 40–54, 2006.

Yu AJ, Dayan P. Uncertainty, neuromodulation, and attention. *Neuron* 46: 681–692, 2005.

Zenger-Landolt B, Heeger DJ. Response suppression in V1 agrees with psychophysics of surround masking. *J Neurosci* 23: 6884–6893, 2003.

Zhou M, Liang F, Xiong XR, Li L, Li H, Xiao Z, Tao HW, Zhang LI. Scaling down of balanced excitation and inhibition by active behavioral states in auditory cortex. *Nat Neurosci* 17: 841–850, 2014.

Zohary E, Shadlen MN, Newsome WT. Correlated neuronal discharge rate and its implications for psychophysical performance. *Nature* 370: 140–143, 1994.